CINTAL - Centro de Investigação Tecnológica do Algarve

Universidade do Algarve

Random Array of Drifting Acoustic Receivers

(RADAR'07)

C. Soares, S. M. Jesus, P. Hursky, T. Folegot,

C. Martins, F. Zabel, L. Quaresma,

Dong-Shan Ko and E. F. Coelho

Rep 04/07 - SiPLAB
15/December/2007

University of Algarve
Campus de Gambelas
8005-139, Faro
Portugal

tel: +351-289800131
fax: +351-289864258
cintal@ualg.pt
www.ualg.pt/cintal

Work requested by	CINTAL - Centro de Investigação Tecnológica do Algarve Campus de Gambelas, Universidade do Algarve 8005-139 Faro, Portugal Tel: +351-289800131, cintal@ualg.pt
Laboratory performing the work	SiPLAB - Signal Processing Laboratory Universidade do Algarve, FCT, Campus de Gambelas, 8005-139 Faro, Portugal tel: +351-289800949, fax: +351-289800066 info@siplab.uceh.ualg.pt, www.ualg.pt/siplab
Projects	RADAR (POCTI/CTA/47719/2002) UAB (POCI/MAR/59008/2004)
Title	Random Array of Drifting Acoustic Receivers 2007 (RADAR07): Acoustic Oceanographic Buoy Data
Authors	C. Soares, S.M. Jesus, T. Folegot, C. Martins and F. Zabel
Date	December 15, 2007
Reference	04/07 - SiPLAB
Number of pages	84 (eighty four)
Abstract	This report describes the complete set of data acquired during the RADAR'07 sea trial, that took place aboard the NRP D. Carlos from July 9 - 15, 2007, off the west coast of Portugal, in the Setúbal area.
Clearance level	UNCLASSIFIED
Distribution list	IH(1), NURC(1), HLS(1), NRL(1), SiPLAB(2), CINTAL (1)
Attached	RADAR07 DVD (1 unit)
Total number of copies	7 (seven)

Approved for publication

S. M. Jesus

General Director

Foreword and Acknowledgment

This report presents the data acquired with two Acoustic Oceanographic Buoy (AOB) systems and the preliminary results obtained during the RADAR'07 sea trial. The RADAR'07 sea trial took place off the west coast of Portugal in the Setúbal area, during the period July 9 - 15, 2007.

The authors of this report would like to thank:

- all the personnel involved, including NRP D. Carlos I crew;
- the support from the involved institutions: Instituto Hidrográfico (IH), NATO Undersea Research Centre (NURC), Naval Research Laboratory (NRL) and Heat Light and Sound Research (HLS);
- FCT (Portugal) for the funding provided under projects UAB (POCI/MAR/59008/2004) and RADAR (POCTI/CTA/47719/2002).

intentionally blank

Contents

List of Figures

intentionally blank

Abstract

The project "Random Array of Drifting Acoustic Receivers" (RADAR) started in 2004 with the objective of developing a network of drifting acoustic-oceanographic buoys (AOBs) for ocean observation. During this project a receiving buoy prototype was developed and tested at sea in 2005 (MakaiEx). During 2006 a second prototype was produced for implementing the network tomography concept, tested at sea during April/May 2007 in the MREA/BP'07 and now in the RADAR'07 sea trial from 9 to 15 July. The conceptual idea is to explore the spatially coherent capabilities of a series of vertical arrays at known positions and its ability to resolve the 3D temperature field along time both with known active sources and possibly with sources of opportunity. The slow movement of the receivers with time, uncertainty of source - receivers relative geometry and evolution through a potentially poorly known bathymetry are the main challenges faced by the inversion of the acoustic data for environmental parameters. Another requirement is that acoustic inversion should be made in nearly real time, or at least, in a time compatible with the evolution of ocean parameters being monitored. The RADAR'07 took place from 9 to 15 July, 2007, in the continental platform, off the west coast of Portugal near the town of Setúbal, approximately 50 km south from Lisbon and involved the oceanographic ship NRP D. Carlos I, from the Portuguese Navy. The data collected included an extensive CTD survey for ocean circulation modelling, acoustic data covering a wide band from 500 Hz up to 15 kHz, received on the AOBs and on a slim vertical array (SLIVA) and used for network tomography as well as for high-frequency tomography and underwater acoustic communications.

intentionally blank

Chapter 1

Introduction

In todays life we are surrounded by networks: a computer network, a wireless network, a mobile phone network, etc... Actually we feel like being ourselves part of a huge World Wide network! The tendency is that the same networking concept will eventually extend to the ocean, with the objectives of ocean monitoring, exploration and surveillance. There are a number of such initiatives both in Europe (ESONET[1]), North America (Neptune and Orion [2]) and Japan (JAMSTEC) [3]. These are large organizations that have a number of short and long term goals among which: *i)* obtain long time series of oceanographical, biological and geophysical relevant parameters at selected locations, *ii)* be able to monitor those parameters on real (or near) real time and *iii)* correlated observed features from one location to the other to infer wide scale effects such as global warming, ocean circulation, internal tide effects, etc...and this should be done on real time and accessible from anywhere through the internet. So the ultimate goal is to have light, easily deployable systems that record, process and transmit environmental information to land stations for worldwide diffusion to authorized users. The concept proposed and developed under RADAR is to use a field of sonobuoys deployed by ship or aircraft to acoustically remote sense the environmental properties (watercolumn and seafloor) of a given ocean volume for Rapid Environmental Assessment (REA). The acoustic data or environmental data collected at the buoy is telemetered to a processing platform aiming at producing acoustic inversions. The resulting environmental models are integrated with concurrent oceanographic prediction models for nowcasts and forecasts in the given area.

These ideias as well as the hardware and algorithmic requirements for their implementation formed the main objectives of the Acoustic Oceanographic Buoy Joint Research Project (AOB-JRP) launched in 2004 and involving various institutions [4] for a 3 year period. Under this JRP, the Signal Processing Laboratory (SiPLAB) team of the UALG has developed a first prototype version of the AO Buoy - AOB1 - in 2003 [1] and a second version - AOB2 - in 2005 [2]. At various levels of participation among partners, two sea trials took place under this JRP, both organized by NURC, the Maritime Rapid Environmental Assessment (MREA) 2003, in the North Elba area (Italy) [3] and the MREA'04 sea trial off the west coast of Portugal, in the continental platform near the town of Setúbal [4]. During both sea trials the AOB1 was tested and the data gathered was analysed

[1] see web site `www.esonet.org`.

[2] see website `http://www.neptune.washington.edu/`

[3] see website `http://www.jamstec.go.jp/`

[4] participating institutions: Université Libre de Bruxelles (ULB), Universidade do Algarve (UALG), Instituto Hidrográfico (IH), Royal Netherlands Navy College (RNLNC) and the NATO Undersea Research Centre (NURC).

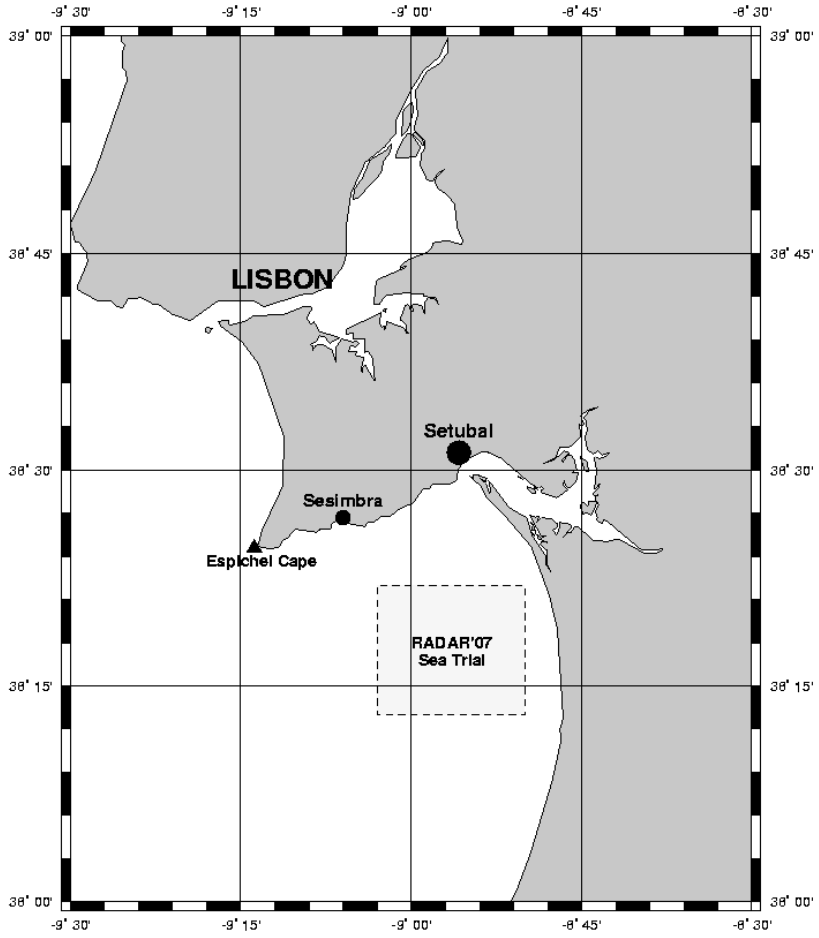

Figure 1.1: *RADAR'07 working area location.*

and results are still being produced and published [5, 6, 7, 8, 9, 10, 11, 12]. AOB2 was first tested during the MakaiEx'05 in the Pacific in the framework of the High Frequency Initiative (HFi) both in high frequency tomography and underwater communications. In 2006 a second unit of the AOB was constructed in order to obtain a network with two nodes. During the RADAR'06 sea trial both of the buoys failed to acquire useful acoustic data for different reasons. Finally, during 2007 both AOBs were successfully deployed in two occasions, one during the MREA/Battle Preparation'07 sea trial, which took place in the Tyrrhenian Sea in April, and during the RADAR'07 aiming at collecting acoustic data with a minimal network of two acoustic receiving devices.

The RADAR'07 sea trial was jointly organized by CINTAL/SiPLAB and Instituto Hidrográfico (IH) with the collaborations of two other teams that were onboard the RV NRP D. Carlos I - from NURC (La Spezia, Italy) and HLS Reasearch, Inc. (San Diego, USA), and a team from the Navy Research Laboratory (NRL) that was responsible for running oceanographic predictions for the experimental area. This sea trial took place in the vicinity of Setúbal in a site located approximately 50 km south of Lisbon, in Portugal, as indicated by the gray box in Fig. 1.1. It served the purpose of collecting acoustic and oceongraphic data for several scientific purposes: (a) low frequency acoustic data (up to

3 kHz) with multiple acoustic receiver arrays in order to support the RADAR project (POCTI/CTA/47719/2002) activities, in particular for fulfilling and supporting tasks 3 and 4; (b) high frequency acoustic data (up to 15 kHz) in order to support the development of a high frequency oceanic tomography concept; (c) to support an underwater communications concept using multiple acoustic receiver arrays; (d) oceanographic data to support ocean circulation modelling. Objective (a) closely follows under the steps of the previous line of the MREA experiments. Besides using multiple acoustic arrays, this sea trial provided an opportunity to test an online inversion software able to download data via wireless from the AOBs, extract the signals of interest, and perform environmental inversion. The development of an operational processing platform is a component of paramount importance in the Acoustic REA concept. Objective (b) comes in line with the High Frequency Initiative and the MakaiEx'05 experiment, aiming at testing a high frequency tomography in an area with significant internal wave activity. The NURC team used a slim vertical array (SLIVA) designed for the reception of high frequency acoustic signals. This sea trial was particularly rich in terms of transmitted signals, as waveforms generated for the different objectives were simultaneously transmitted, either by superposition of different waveforms in the same acoustic source, or by simultaneous deployment of two acoustic sources. This resulted in a highly productive sea trial for all teams on board.

During the RADAR'07 sea trial also extensive concurrent oceanographic measurements were performed with a CTD, ADCPs, moored thermistor strings, and a thermistor string colocated with one of the AOB arrays.

The present document aims at providing as much as possible a complete report of the various data sets acquired during the RADAR'07 sea trial both for acoustic and non-acoustic data as well as accompanying relevant information such as ship's and buoys' position, currents, temperature profiles, geo-acoustic information and other concurrent remote sensing data. The companion DVD contains all the basic data and respective master routines for data manipulation and pre-processing. This report is organized as follows: chapter 2 reports on all the non-acoustic data such as environmental data geometries of intruments during the RADAR'07 sea trial; chapter 3 is dedicated to the acoustic data describing the instrumentation used to transmit and collect signals, and describes transmission schedules throughout the experiment; chapter 4 briefly describes the computational facilities available on board, and reports on the inversion of acoustic data inversions carried out during the sea trial; finally section 5 concludes this report giving some hints about most interesting sets for posterior processing. Additionally, appendix sections were describing in detail files and routines used to generate waveforms included in the different transmission lineups composed for the sea trial.

Chapter 2

The RADAR'07 sea trial

2.1 Generalities and sea trial area

The selected area for the RADAR'07 sea trial is shown in figure 2.1 together with the transects A-B, A-C, A-D, A-E planned for acoustic transmissions and geophysical observations. There a number of interesting features in this area for performing shallow water experiments: in a small area within 10 km it encompasses a large range-independent platform at 120 m depth, a slowly range-dependent variable bottom to the coast, a highly range-dependent bottom to offshore, and a huge submarine depression on the continental platform: the submarine canyon of Setúbal; it is an area with a known and well documented internal wave activity [13] and therefore potential generator of oceanographic - acoustic relevant features; logistically convenient for its vicinity to the base port of Lisboa and last, but not least, well protected from north winds and sea waves by the Espichel Cape (see general view in Fig. 1.1).

This is a well documented area where at least three acoustic cruises took place in the last 10 years. There were a number of geological and oceanographic surveys carried out in connection with those or other sea trials, in the area. Bathymetry and the nature of the bottom is also well known and regularly surveyed since this is the approach for the busy port of Setúbal served by a number of container lines and shipyards. In this period of the year the weather is generally calm dominated by north/northwest winds sometimes up to 10/15 knot, picking up in the afternoon and reducing during the evening. There is a strong tidal influence that induces the known ellipsoidal current bi-diurnal cycling drawing some influence of fresh water from the Sado river mouth in Setúbal (see [14] for details on salinity variations in the area).

During the testing the sea was relatively calm varying from sea state 2 in first day and then progressively reducing during the week to sea state 1 and 0. Currents and wave height information was gathered by the bottom mounted ADCP measurements made at two locations (see section 2.2.2). During the RADAR'07 sea trial there were quite extensive measurements of the water column temperature and salinity in order to obtain a ground truth for data inversion validation (see section 2.2.2). Two research vessels were involved in the operations: the NRP D. Carlos I and the NRP Auriga (for equipment recovery on July 16, 2007) from the Portuguese Navy, leaded by Instituto Hidrográfico, partner in the RADAR project and task leader for sea experiments.

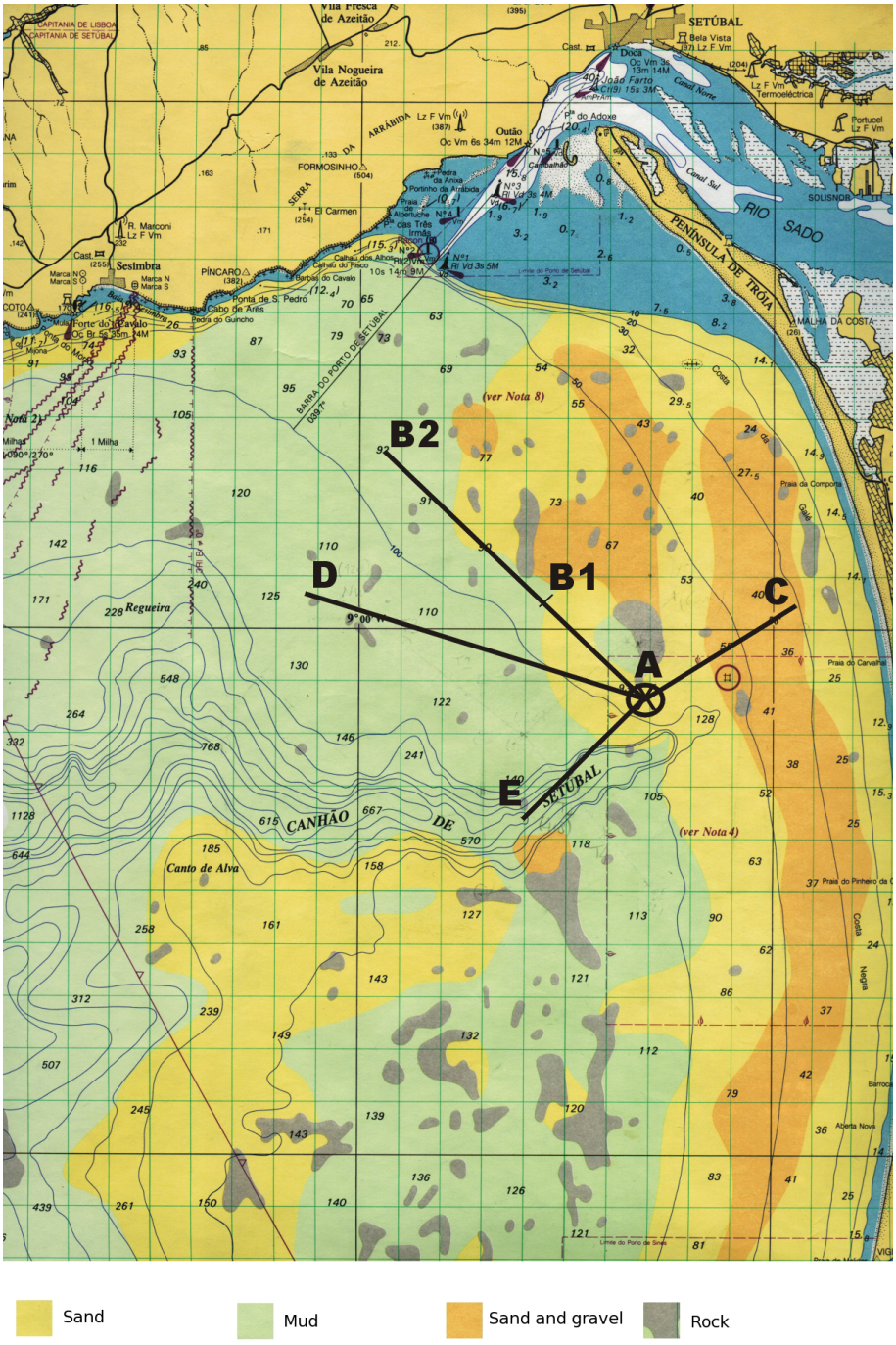

Figure 2.1: *RADAR experiment area off the west coast of Portugal in the continental platform in front of the Tróia Peninsula: transects A-B,C,D and E.*

2.2 Ground truth measurements

The working box is located in a pretty well known area where several previous sea trials took place: INTIMATE'99 in July 1999 with NRP D. Carlos I, INTIFANTE'00 in October 2000 with NRP D. Carlos I and NRP Auriga under projects INTIMATE and INFANTE [15] and MREA'04 in April - May 2004 with the NRV Alliance, organized by NURC [4]. There are several attractive features in this area: one is that this is a relatively protected

area from North winds, which might be particularly violent in the west coast of Portugal; the other is that it has only 5 hours transit time from the naval basis in Lisbon; embark and disembark of personnel can easily be done at Sesimbra; and finally, in case of need, a shelter port is available in Setúbal, where the portuguese navy has a dedicated pier.

From the oceanographic point of view this area has a significant internal tide activity due to the presence of bathymetric features such as the Setúbal canyon which approaches Setúbal Bay, seamounts situated on the continental slope, and a narrow continental shelf. Further into the deep ocean a group of seamounts (Horseshoe, at around 11°W, 37°N) rise up to 200 m from the abyssal plain. The region is also known for upwelling events, frequently observed in summer owing to the prevailing northerly winds [16].

2.2.1 Bottom data

For the RADAR'07 experimental area no archival bottom data was available. The only reference for bottom materials is the map in Fig. 2.1, roughly indicating which materials are found over the experimental area. According to that map point A is located in a position of sandy seafloor (yellow), points B2, D and E are located in muddy seafloor sites (green), and C is located over sand and gravel (orange). This map provides only an approximate classification.

2.2.2 Water column data

As mentioned above a set of water-column measurements were performed during RADAR'07, including standard CTD casts from NRP D. Carlos I, two thermistor strings (TS1 and TS2), autonomous recording temperature sensors on SLIVA, drifting thermistor strings colocated with the vertical arrays on the AOBs and two bottom mounted ADCPs.

CTD casts

There were a number of CTD casts performed from NRP D. Carlos I during night shifts. All cast locations are shown in figure 2.2. It can be noticed that for validation purpose, several locations were probed twice during the sea trial. The actual CTD casts data made from NRP D. Carlos I are shown in figure 2.3 for the temperature profiles (a) and for the salinity profiles (b), where the black thick curve represents the mean profile. A pronounced thermocline of 4°C can be observed extending down to 40 m depth, with a strong variation over the whole data set, in the period and area of interest. The mean profile thermocline is around 20 m depth, so the variations to 40 m are possibly due to internal wave activity. This can be better observed in the thermistor string data below.

Moored instrumentation

At the beginning of the sea trial two thermistor strings and two ADCPs were deployed by IH and NURC, each with one of them. The SLIVA acoustic reception system was deployed during Julian day 191. Figure 2.4 shows the positions of these instruments on a bathymetry map.

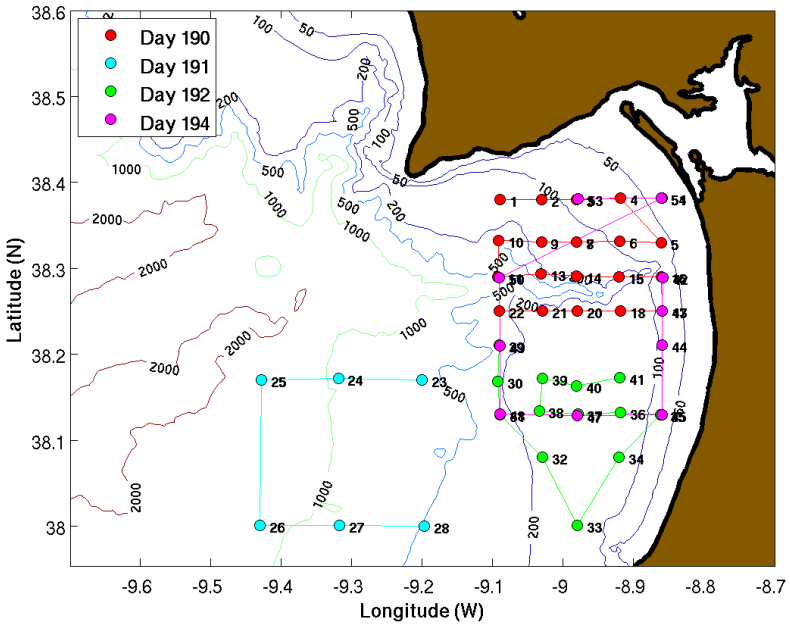

Figure 2.2: *CTD locations performed by NRP D. Carlos I during RADAR'07.*

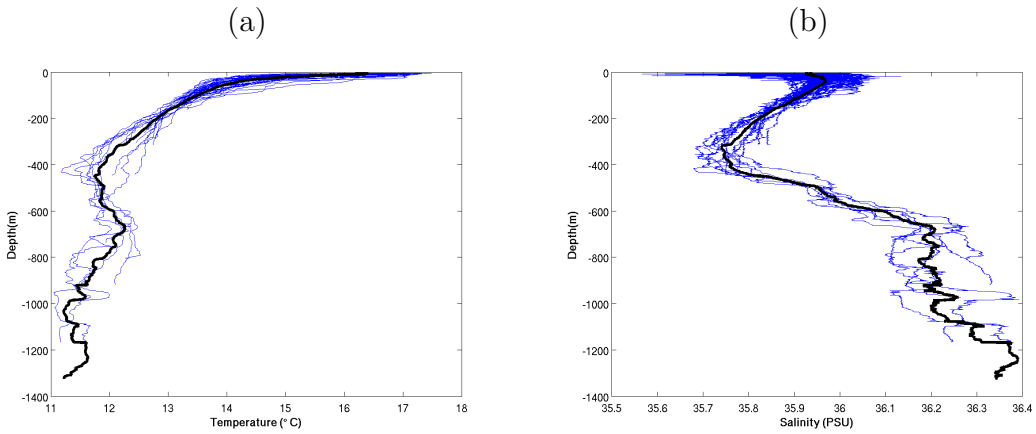

Figure 2.3: *recorded CTD casts from NRP D. Carlos I between July 9 and July 14, 2007: temperature profiles (a) and salinity profiles (b). The black thick curve is the mean profile.*

The thermistor strings were installed at positions to the south and to the north of line AB as shown in figure 2.4. The SLIVA reception system was deployed at point A. Table 2.1 indicates deployment coordinates and respective water depths. The thermistor depths of the IH string are 2 to 22 m with a spacing of 2 m. The deepest sensor did not work properly and was discarded. The thermistor depths of the NURC string are 15 to 99 m with a spacing of 1 m, hence there is a depth overlapping. Figure 2.5 shows the temperature measurements obtained with the IH and NURC thermistor strings. Similar temperature values and variations can be observed at the top thermistors of the NURC string and at the bottom of the IH string, with a slight delay at the IH thermistor string. The internal tides activity can be clearly observed as the thermocline's depth has a semi-diurnal variation. It can be also noticed in both plots that the temperature at the surface increased as time elapsed.

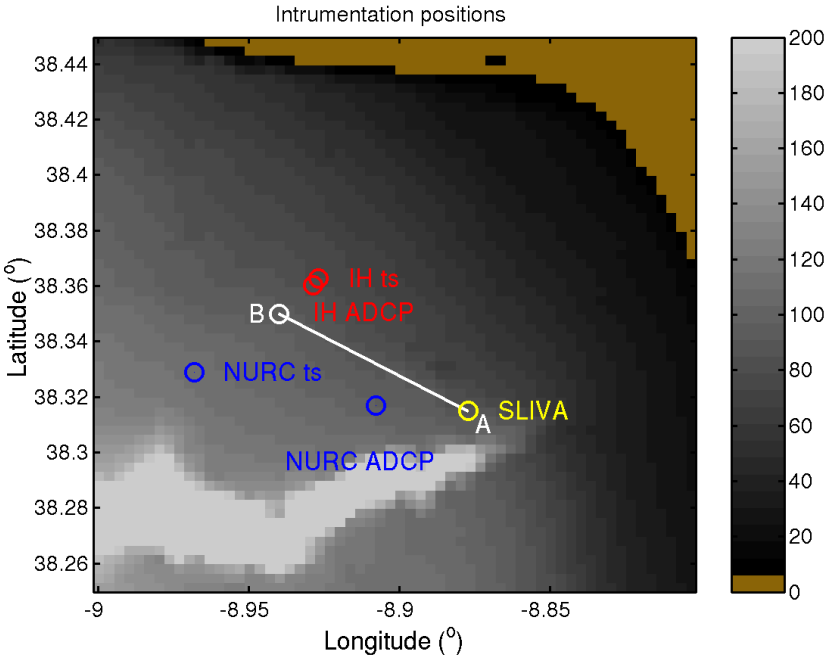

Figure 2.4: *RADAR'07 bathymetry map with thermistor strings', ADCPs', and SLIVA's locations. SLIVA was deployed at point A.*

	Longitude (deg)	Latitude (deg)	Water depth (m)
NURC thermistor string	8.9682W	38.3288N	115
NURC ADCP	8.9078W	38.3168N	100
IH thermistor string	8.9270W	38.3626N	82
IH ADCP	8.9287W	38.3604N	80
SLIVA	8.8773W	38.3150N	89.5

Table 2.1: Deployment coordinates of moored instrumentation - thermistor strings, ADCPs, and SLIVA - with respective water depths.

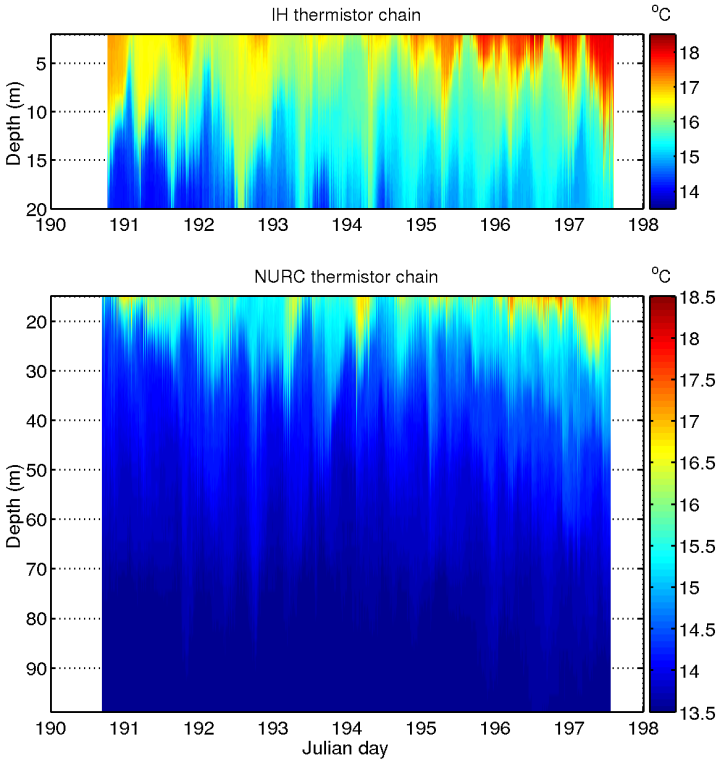

Figure 2.5: *Temperature data collected with the IH and NURC thermistor strings covering the whole duration of the RADAR'07 sea trial.*

AOB thermistor strings

The AOB22 was fitted with a low precision digital array of 16 temperature sensors. The array structure and details are described in [17] but in short this is a series of 0.5 ° C precision sensors sampled at 4 s with 12-bit resolution. The data was lowpass filtered with a moving average filter and a window size of 50 samples, which produces an approximate cutoff frequency of 5 mHz. The T sensors are colocated with the hydrophones so they start at 6.6 m depth and have a constant interval of 4 m. The recordings are shown in figure 2.6 for deployment days 192 to 195. This data clearly shows a strong internal wave activity, specially at the beginning of the recording of day 193, where the thermocline is seen to exceptionaly extend down to nearly 40 m. As observed with the IH and NURC thermistor strings, also with these thermistor data it is observed that surface tamperature increases through days 192 to 195.

Autonomous T sensors

Autonomous temperature sensors were place along the mooring line of SLIVA and were recovered at the end of the experiment. This data is available in a companion report by NURC.

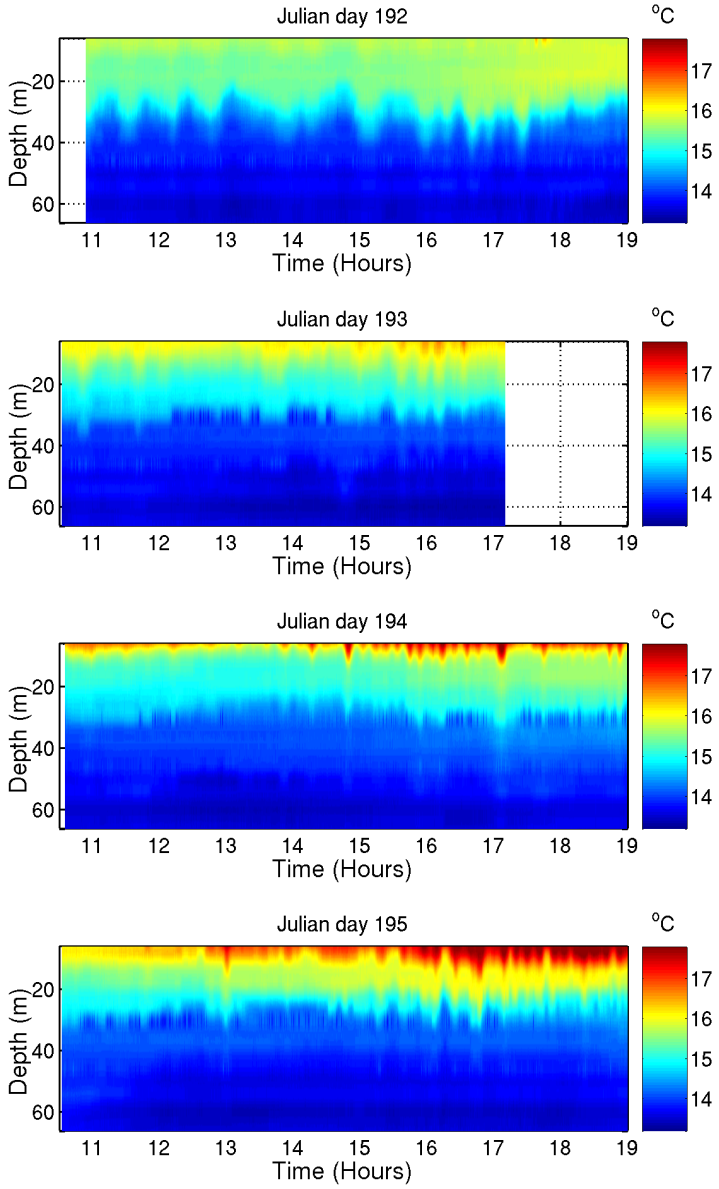

Figure 2.6: *AOB22 thermistor string data for deployment days 192, 193, 194 and 195.*

Empirical Orthogonal Functions

The orthogonal decomposition of the CTD temperature data over depth according to

$$\hat{T}(z) = \bar{T}(z) + \sum_{i=1}^{N} \alpha_i U_i(z), \qquad 0 \leq z \leq H \tag{2.1}$$

where α_i are the EOF coefficients, $U_i(z)$ the EOF's and H is the water depth, chosen equal to a minimum of 120 m (Fig. 2.7) in this example gave a set of EOF's which first three are shown in figure 2.7(b) and are meant to represent more than 95% of the total energy in the water column. In order to obtain this decomposition the CTD data were interpolated at every meter between 3 and 100 m depth. A total of 35 profiles were used for this calculation.

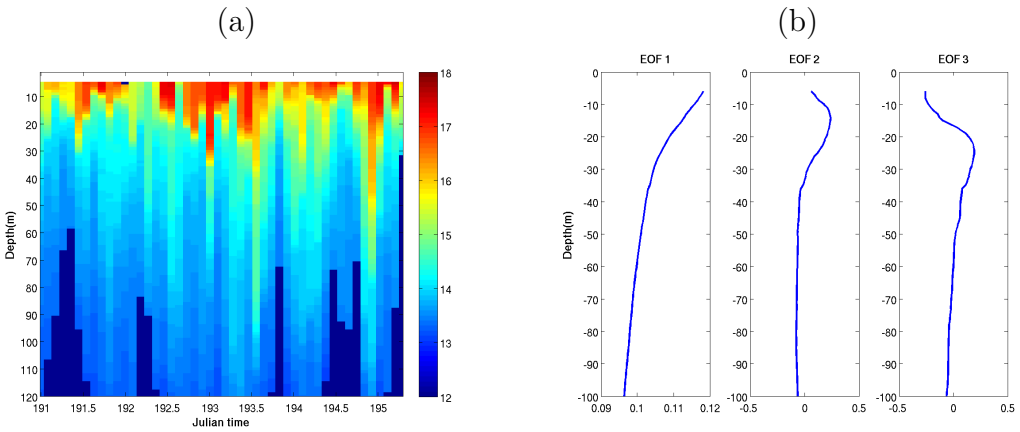

Figure 2.7: *all CTD data upto 120 m depth (a) first three EOF's computed from CTD data up to 100 m depth (b).*

Current data

Also two ADCPs were moored at the beginning of the sea trial, one by IH and the other by NURC, at coordinates indicated in table 2.1. Figure 2.8 shows the current data collected with ADCP provided by IH, with Fig. 2.8(a) showing absolute current velocity; Fig. 2.8(b) showing the North-South component, and 2.8(c) showing the East-West component. Figure 2.9 shows a stick diagramm representing the current data collected by NURC. The stick indicates the current direction and velocity. These data show that currents are in phase with tide, and show that the current velocity is in average about 0.1 m/s, with maximum values of 0.25 m/s.

2.3 Ocenographic prediction

During the RADAR'07 sea trial, NRL produced oceanographic predicitons for the experimental area on watercolumn temperature and salinity, surface temperature and salinity. In particular, predicitions for the cross-sections from points A to B, A to C, A to D, and A to E, and cross-sections on latitude 38.28N and longitude 9.00W, among others, were obtained. Figure 2.10 shows an example of temperature forecasts over the cross-sections from point A to B through E for Julian day 193 obtained 12 hours ahead. These predicitions were based on Multichannel Sea Surface Temperature (MCSST) measurements and satellite altimeter data. No in-situ measurements were used. As an example, Fig 2.11 shows predictions for the same day at the sea surface and at 50 m depth for same area [1].

2.4 Deployment geometries

AOB21 and AOB22 deployments during RADAR'07 were all in free drifting configuration as reported in table 2.2 where the experiment type and acoustic transmissions are also mentioned.

[1]The NRL internet site contains predictions for this area from days July 1, 2008 to July 25, 2008, at `http://www7320.nrlssc.navy.mil/MREA04/RADAR07_WWW/RADAR.html`

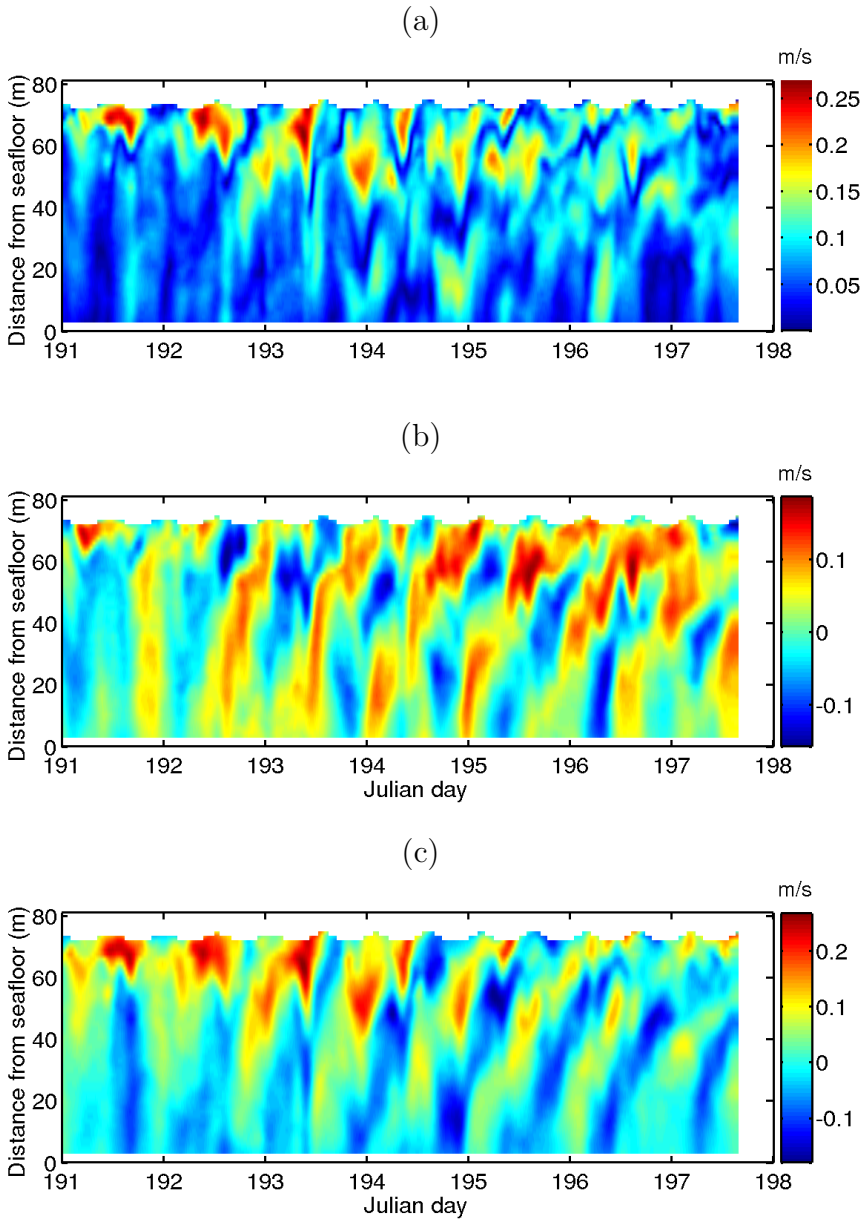

Figure 2.8: *Currents measured with the IH ADCP: Absolute current values (a); North-South component (b); East-West component (c). The blank portions denote depth and times where there is no data.*

Year day	Julian	AOB2	Experiment	Transmissions
Wed July 11	192	1 & 2	test and preparation	LF,MF,HF
Thu July 12	193	1 & 2	24h HF tomography	LF,MF,HF
Fri July 13	194	1 & 2	underwater comms	LF,MF,HF
Sat July 14	195	1 & 2	network tomography	LF,MF,HF

Table 2.2: *Acoustic Oceanographic Buoy (AOB) deployments during RADAR'07.*

2.4.1 Acoustic source depth

Active signals were transmitted from NRP D. Carlos I with three sound sources: a low frequency (LF) Lubell source covering the band 500 to 4000 Hz, a medium frequency

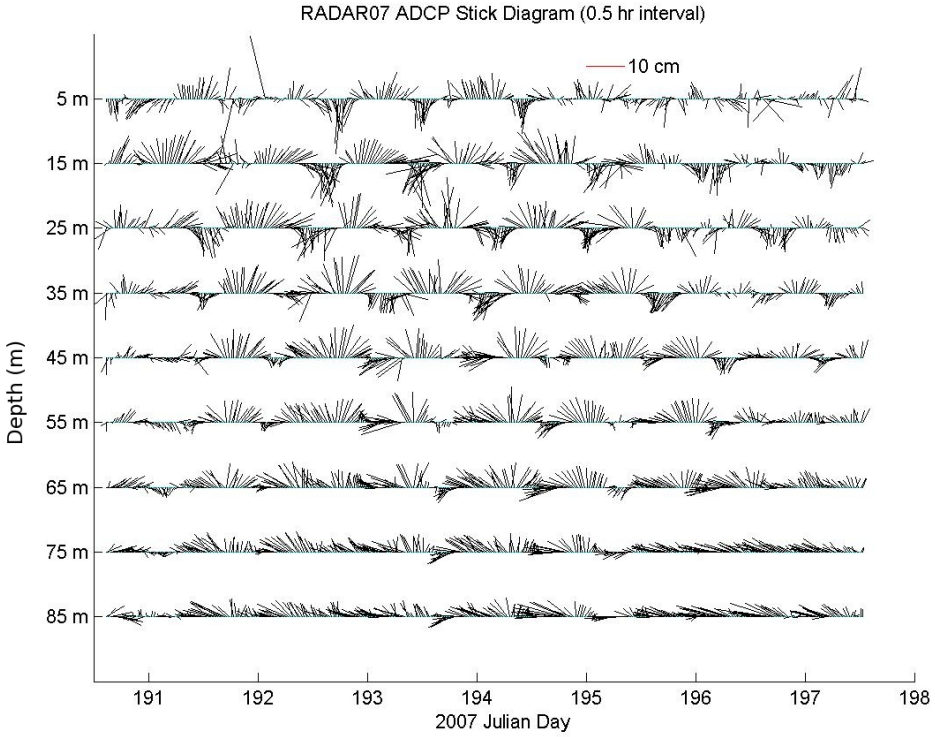

Figure 2.9: *Currents measured with the NURC ADCP represented by a stick diagram. The sticks indicate current amplitude and direction.*

(MF) source covering 4 to 8 kHz and an high frequency (HF) source transmitting in the band 11 to 20 kHz. The MF and HF sources were mounted on the same frame so there was a unique depth reader. The Lubell source was limited in depth while the MF/HF pair had no depth limitations. During the experiment the NRP D. Carlos I was either on station or under tow while transmitting pre-coded acoustic signals.

MF/HF source

Figure 2.12 shows in the upper plot the depth recording of the MF/HF source and the lower plot the respective temperature. Blue curves indicate that the AOBs were deployed, while lightblue curves indicate intervals after AOBs recovery. The upper plot shows the depths of the MF/HF acoustic source during the deployments of the AOBs. Day 193 was dedicated to HF tomography. During this day the MF/HF source was deployed at 70 m depth during the whole experiment, which was called *deep run*. The period in between the blue and the lightblue curve segments was used for AOBs recovery and SLIVA disk change. During day 194, dedicated underwater communications, the MF/HF source was first deployed shallow with nominal depth of 14.4 m (called *shallow run*); then it was deployed deep at 60 m; and then it was deployed shallow again at 10 m, as shown in the upper plot. During the deep run several depth variations are noticeable which is caused by movement of the RV. During shallow runs such movements do not significantly change the source depth. Finally, during day 195, dedicated to networked tomography, the MF/HF was first deployed deep at 60 m depth, and then shallow at 10 m depth. During the *deep run* several variations between in source depth are noticed: during this experiment the source was towed between several stations. After the network tomography experiment the

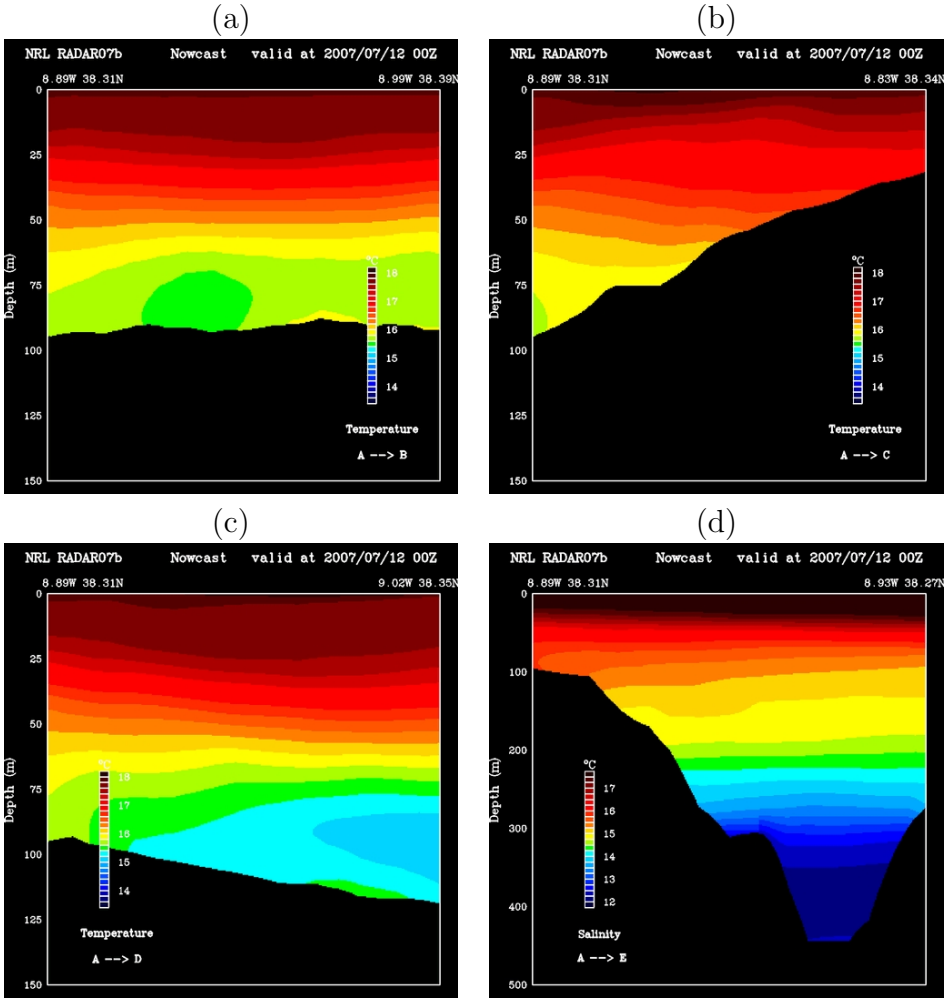

Figure 2.10: *Cross-section temperature predictions over cross-section A-B (a); A-C (b); A-D (c); and A-E (d).*

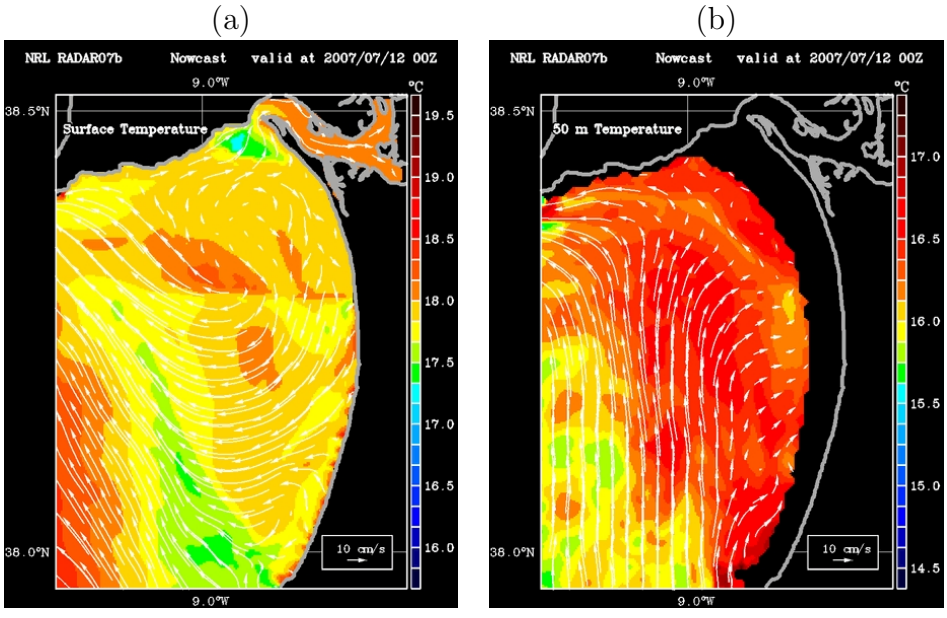

Figure 2.11: *Surface temperature predition (a) and 50 m depth temperature prediction (b).*

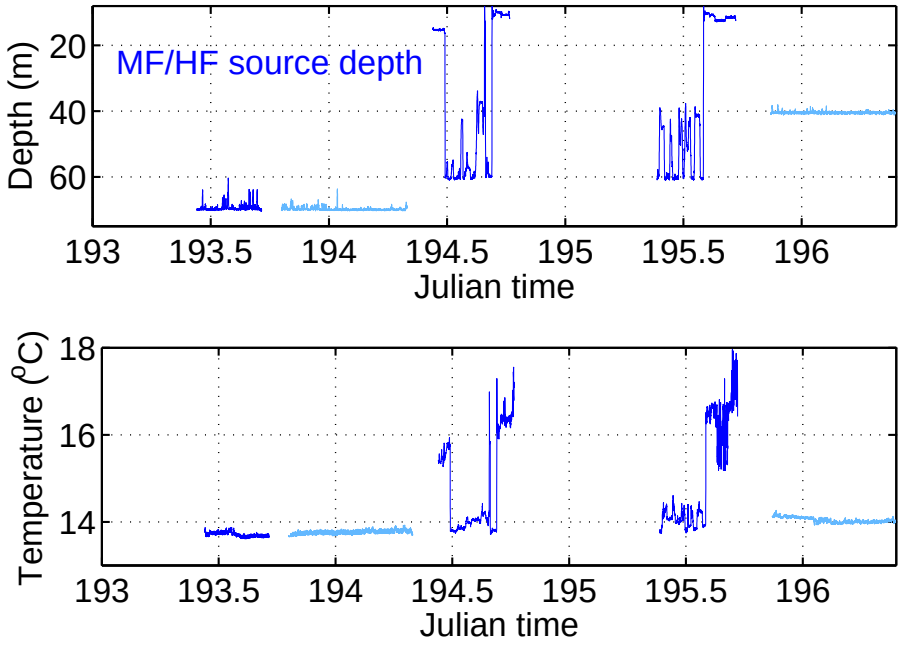

Figure 2.12: *MF/HF source depth (upper plot) and temperature (lower plot) recordings. Lightblue color indicates intervals after AOBs recovery.*

Julian day	GMT time	Depth (m)
193	09:07	70
193	19:11	70
194	10:13	14
194	11:48	60
194	16:32	10
195	09:00	60
195	14:06	10
195	20:52	40

Table 2.3: Time table presenting times of MF/HF source transmission start and nominal depths .

MF/HF source deployed at a nominal depth of 40 m for a 12-hours range-dependent high-frequency tomography run. Table 2.3 presents a summary of the MF/HF deployments over days 193 through 195 indicating times of transmission starts and nominal source depth.

Together with the depth sensor was included also a temperature sensor which recorded the water temperature at the source depth. The lower plot of Fig. 2.12 shows that a decrease in source depth is accompanied by a rise in the temperature value, with a variation between 13.8^oC at 70 m depth and 18^oC at 10 m depth.

LF Lubell source

Figure 2.13 shows in the upper plot the depth recording of the Lubell source and in the lower plot the respective temperature for days 193, 194 and 195.

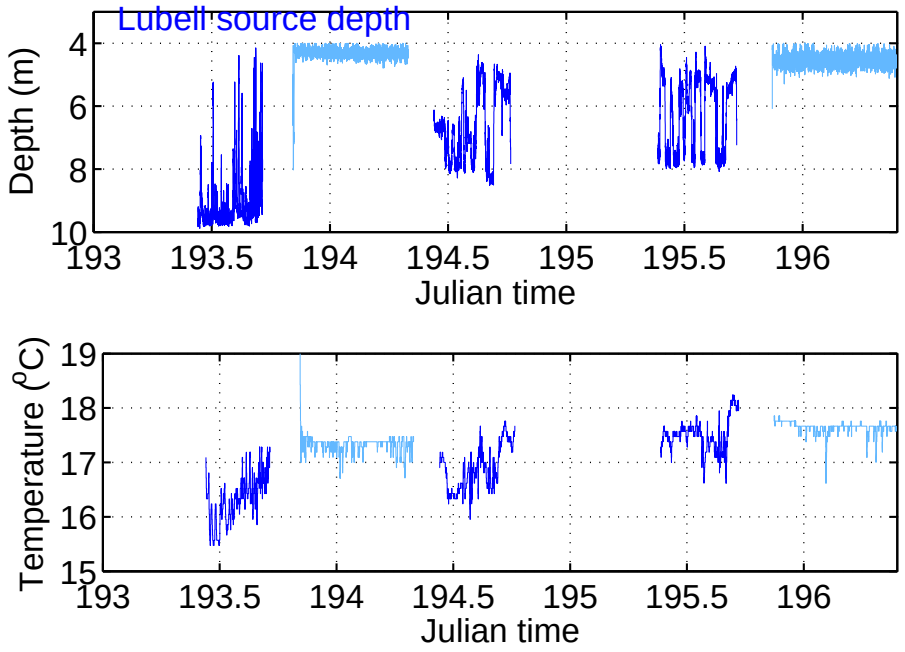

Figure 2.13: *LF Lubell source depth (upper plot) and temperature (lower plot) recordings during deployments of Julian days 193, 194 and 195. Lightblue color indicates intervals after AOBs' recovery.*

During day 193 the Lubell transducer was deployed with nominal depth of approximately 10 m. Variations in depth between 4 and 10 m are observed in close relation to tow speed. The period in between the blue and the lightblue curve segments was used for AOBs recovery and SLIVA disk change. For the run at night (lightblue curve) the Lubell source was initially deployed at a depth of 8 m, and then a at a depth between 4 and 5 m. During day 194 and 195 the nominal deployment depth was 8 m, while the depth variability is between 4 and 8 m. The depth curve of day 195 clearly allows to identify an alternation between tows and stations performed during the network tomography run. During the range-dependent tomography run the Lubell source was deployed at a depth between 4 and 5 m.

Attached to this acoustic source was also a temperature sensor. In this case temperature variations of less than 2^oC are observed at each day. These variations are rather attributed to temperature variations over time and geographic coordinates than to temperature variations over depth.

2.4.2 AOBs receiver depth recordings

In order to obtain a direct measurement of the AOBs' receiver depths through time and their dependence on surface motion, one depth recorder was installed on each array. Figure 2.14 shows depth (a) and (b) and water temperature (c) and (d) recordings for AOB21 (left) and for AOB22 (right). During the deployment of day 192, the recorders were placed for both arrays together at hydrophone 2, which roughly corresponds to 15 m for AOB21 and to 10.3 m for AOB22. No recording exists for day 193 while for day 194 the recorders were now placed at the level of hydrophone 1: 10 m for AOB21 and 6.3 m for AOB22. During day 195 there was a clear increase of oscillation by the end of the recording. Temperature recordings are in agreement with the expectations for those

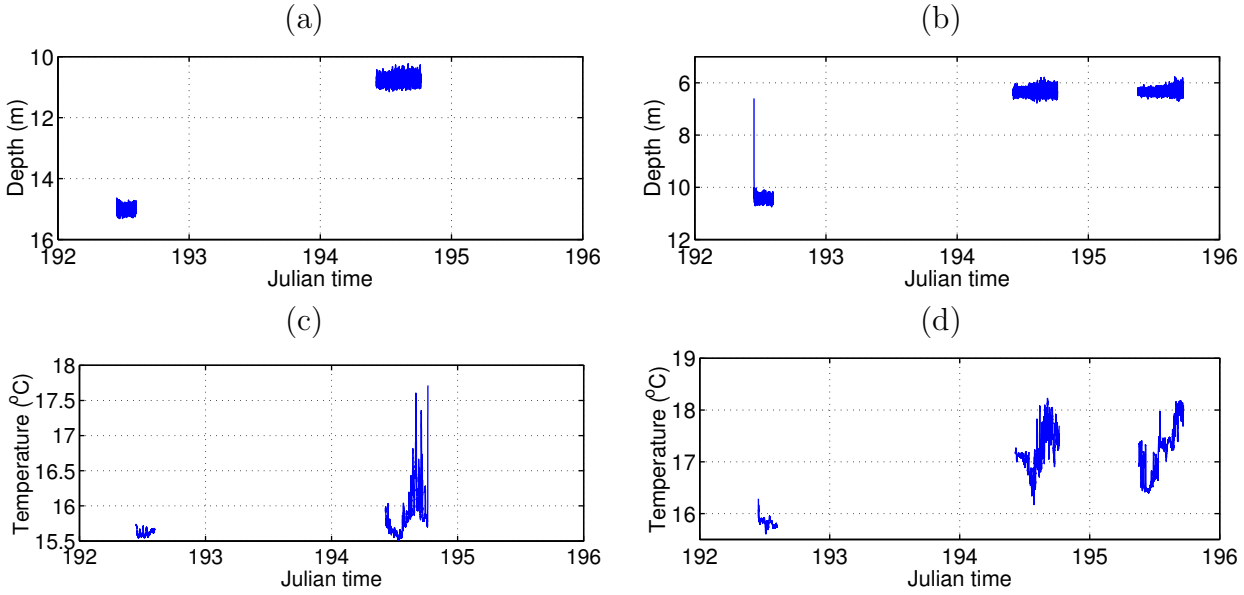

Figure 2.14: *Array depth oscillations, (a) and (b), and temperature recordings (c) and (d), through time for AOB21 (left) and for AOB22 (right).*

depths (thermocline).

2.4.3 Drift during day 192 (July 11, 2007)

The two AOBs were deployed on day 192 at the locations shown in figure 2.15(a), that also shows their drifts during the whole deployment together with NRP D. Carlos I track. The sound sources were deployed soon after the deployment of the second AOB and transmissions have started and lasted for less than 4 hours. Source receiver range, shown in figure 2.15(b), has varied between 1 and 5 km during the acoustic transmission. Figure 2.15(c) shows the drift velocities, which were smaller than 0.1 m/s. The original GPS data was lowpass filtered by a moving average filter with a window size of 12 samples ($\approx$ 2 minutes).

2.4.4 Drift during day 193 (July 12, 2007)

The second day was dedicated to the high frequency tomography 24 h run that started early in the morning after the deployment of the two AOBs. During the whole day the source ship remained on station as shown in figure 2.16 giving rise to the source -receiver distance as shown in figure 2.16. It remained almost constant thanks to a drifting direction of AOB22 that is perpendicular to the plane including AOB22 and the acoustic source. The drift velocity during this day recorded by the GPS system of AOB22 was less than 0.1 m/s. The GPS system on AOB21 failed and therefore the position is not availlable for this drift. The curves presented in figure 2.16 assume that AOB21 drifted away from the initial position exactly in the same manner as AOB22.

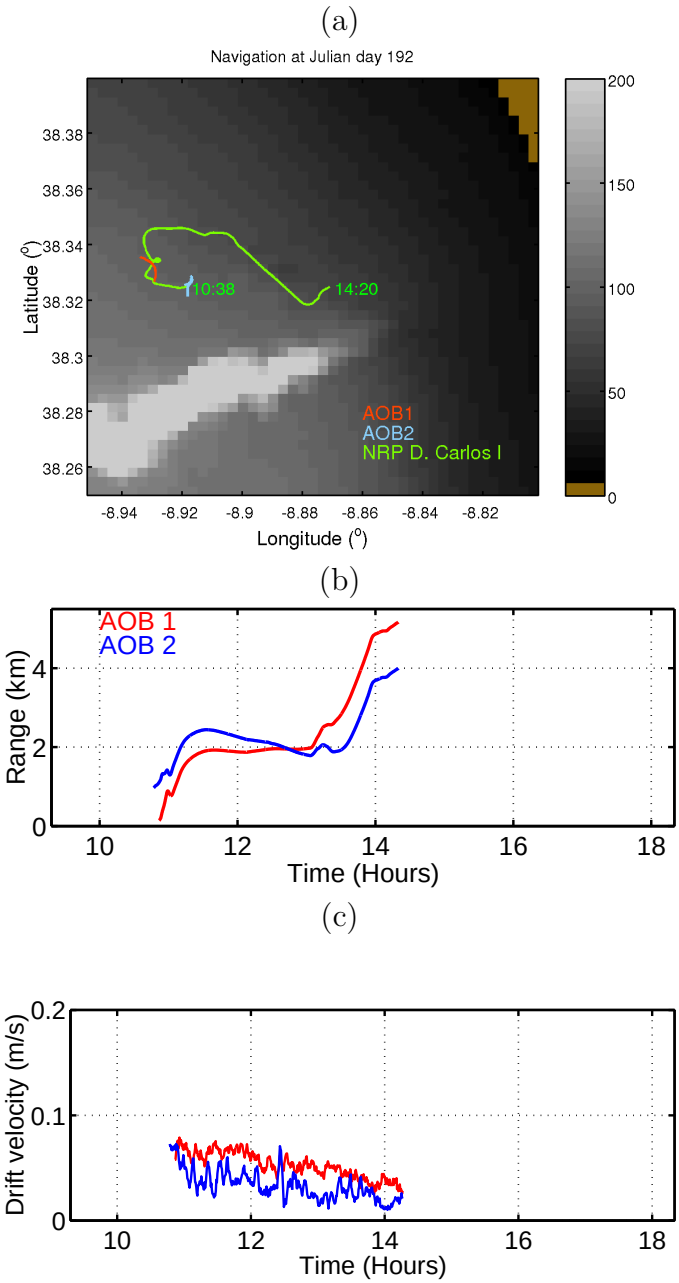

Figure 2.15: *GPS estimated AOB21 and AOB22 drift, NRP D. Carlos I tracks during day 192 (a); GPS estimated AOB21 and AOB22 range from NRP D. Carlos I during day 192 (b); GPS estimated AOBs' drift velocity during day 192 (c).*

2.4.5 Drift during day 194 (July 13, 2007)

This day was dedicated to underwater communications so the two AOBs were deployed at the locations shown in figure 2.17(a), that also shows their drifts during the whole deployment together with NRP D. Carlos I track. The sound sources were deployed soon after the deployment of the second AOB and transmissions have started and lasted for about 6 hours. The track performed by research vessel was such that different ranges and range-dependencies with bathymetry could be obtained. Source receiver range is shown in figure 2.17(b), attaining a maximum of 5.2 km. Finally, figure 2.17(c) shows the AOB drift velocity which is about 0.1 m/s.

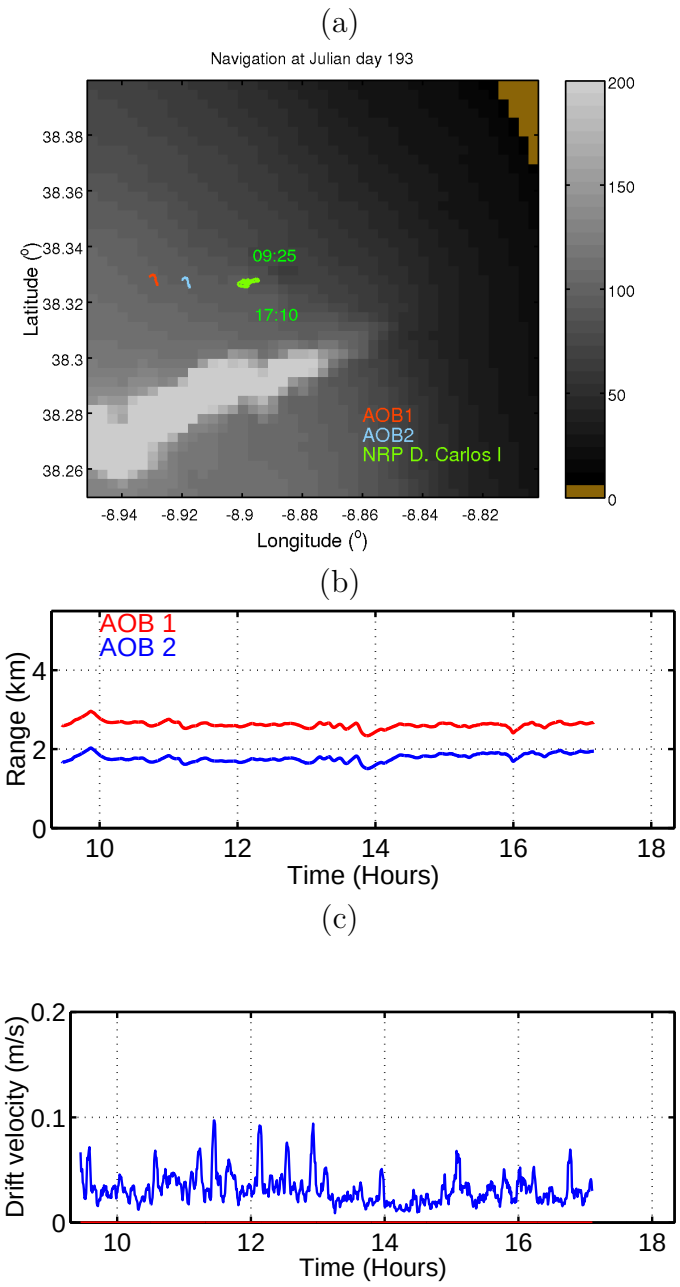

Figure 2.16: *GPS estimated AOB21 and AOB22 drift, NRP D. Carlos I tracks during day 193 (a); GPS estimated AOB21 and AOB22 range from NRP D. Carlos I during day 193 (b); GPS estimated AOBs' drift velocity during day 193 (c).*

During day 194 there were also stations where the RV held its position during a certain time. Table 2.4 indicates approximate coordinates and time intervals of stations held during this day.

2.4.6 Drift during day 195 (July 14, 2007)

This day was finally dedicated to network tomography where the two AOBs were deployed in the vicinity of SLIVA and in the center of a large circle around which the sound source was navigating. This is shown in figure 2.18(a) for the AOBs and ship tracks, and in

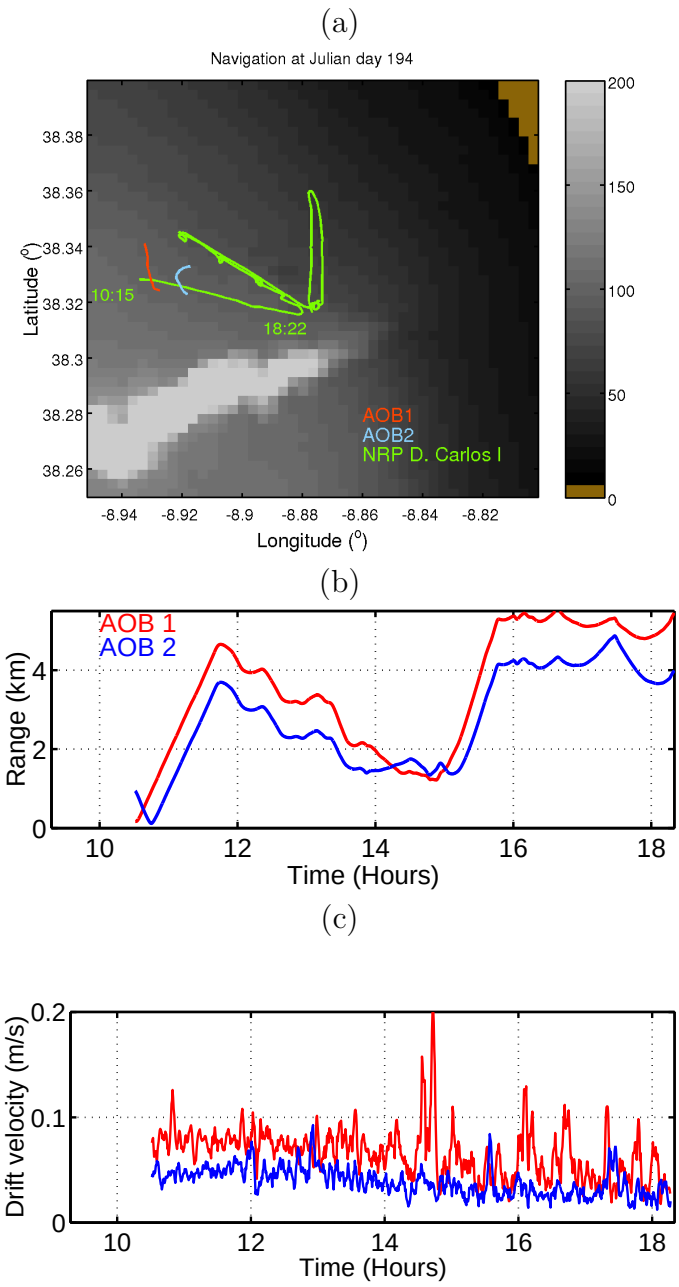

Figure 2.17: *GPS estimated AOB21 and AOB22 drift, NRP D. Carlos I tracks during day 194 (a); GPS estimated AOB21 and AOB22 range from NRP D. Carlos I during day 194 (b); GPS estimated AOBs' drift velocity during day 194 (c).*

figure 2.18(b) for source receivers range, which attained about 5 km. Table 2.5 indicates the stations performed with start and stop time and approximate coordinates. Figure 2.18(c) shows the drift velocity which is close to zero during the morning and reaches 0.4 m/s during the afternoon.

Longitude	Latitude	Start time	Stop time
-8.895	38.327	12:42	13:15
-8.920	38.343	14:27	14:48
-8.875	38.319	15:48	16:36

Table 2.4: Approximate coordinates and times of the stations held by RV D. Carlos I during day 194.

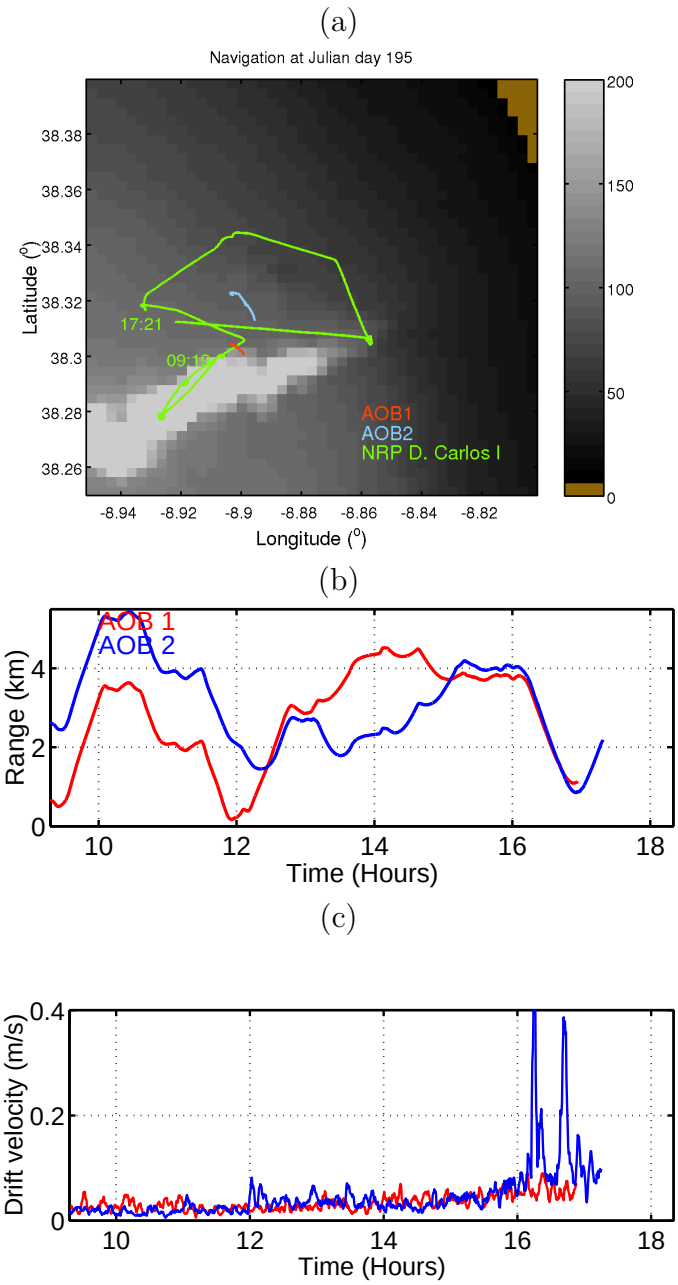

Figure 2.18: *GPS estimated AOB21 and AOB22 drift, NRP D. Carlos I tracks during day 195 (a); GPS estimated AOB21 and AOB22 range from NRP D. Carlos I during day 195 (b); GPS estimated AOBs' drift velocity during day 195 (c).*

Longitude	Latitude	Start time	Stop time
-8.927	38.280	10:06	10:36
-8.920	38.290	10:54	11:30
-8.932	38.316	12:48	13:04
-8.908	38.341	13:40	14:05
-8.857	38.310	15:20	16:05

Table 2.5: Approximate coordinates and times of the stations held by RV D. Carlos I during day 195.

Chapter 3

Acoustic data

Acoustic transmissions performed during RADAR'07 were unique in several senses. The first original point is that different experiments were running in parallel transmitting different signals multiplexed both in time and frequency. This was made possible since there were three independent sound sources transmitting in non overlaping frequency bands and the receiving systems were wide band. This multiplexing in time and frequency required a flexible signal generation capacity that in RADAR'07 was achieved with three independent generators, one of which could drive two channels. It is therefore very important to accurately describe the characteristics and particularities of each generator and signal transmitted on each phase of the experiment so as to allow for the processing of the received signals in the best conditions (see section 3.3).

Active signals were transmitted from NRP D. Carlos I either by towing acoustic sources or on stations. These signals were covering the band between 0.5 to 20 kHz, for tomography, linear frequency modulated (LFM) chirps, tones, pseudo-random noise (PRN) sequences, and for communications, phase shift keying (PSK) and frequency shift keying (FSK) modulations, and OFDM waveforms. This section is dedicated to the signal emission first by describing the hardware system and then the actual emitted signals' waveforms.

The transmitted signals were received also on three separated systems : the SLIm Vertical Array (SLIVA) that was moored on (or near) point A and the two AOBs: AOB21 and AOB22 that were drifting in the area in positions and ranges as shown in section 2.4.

3.1 Signal generators

3.1.1 The UALG signal generation system

The UALG team used a signal generation system consisting of a PC with a 12 bit Da tum digital-to-analog converter (DAC) serving a Lubell 1424HP chain (consisting of an attenuator, pre-amplifier, impedance box, and the Lubell acoustic projector itself). The system is fed with a data text file containing integer values ranging from -2048 to 2047 representing the waveform to be transmitted. The sampling frequency may vary from 2.4 Hz to 1 MHz, and the data file may hold up to 50 million data points. The user configures emission starting time and repetition time of the transmission. The system

Julian day	Sampling frequency (Hz)	acoustic projector
192	10000	Lubell
193	96000	ITC pair
194	48000	Lubell
195	48000	Lubell

Table 3.1: Nominal sampling frequencies used in the UALG signal generation system together with acoustic projector over the RADAR'07 acoustic experiments.

uses GPS strobes to start the emission of the waveform at precise times according to previously defined starting and repetition rates.

During RADAR'07 it was found that in some cases the deviation of the effective sampling frequency relative to the nominal frequency was significant. In particular, it was concluded that nominal frequency 48000 Hz is in effect 48019.21 Hz, and 96000 Hz is in effect 96153.84 Hz. The latter constitutes a deviation of about 0.16% and the former constitutes a deviation of about 0.04% which may have a significant impact in underwater communications and high-frequency tomography. This error causes the waveform to be time compressed, i.e., it is shorter than supposed by the experimenter. Although the cause is different, this resembles the Doppler effect, since the signal is being emitted at a different rate than supposed. The waveform suffers a frequency shift and band compression according to this frequency shift. In this case the band will be enlarged and the central frequency increased. For 10 kHz and nominal frequency of 96 kHz the shift is 16 Hz; for 48 kHz sampling frequency the shift is 4 Hz. At low frequency, below 1 kHz the frequency shift is respectively 1.6 and 0.4 Hz. Table 3.1 shows the sampling frequencies used in each day with the respective acoustic projector. During Julian day 192 nominal sampling frequency of 10 kHz was used which is also the effective frequency. The acoustic setup are explained in the next section.

3.1.2 The NURC signal generation system

The NURC signal generation system used a National Instrument generation card. The memory was limited to 25 Msamples, with selectable sample frequencies. The input of the system is a binary file containing the signal to emit. No filter was implemented, besides the natural filters from the amplifier and transducers. The electrical signal at the output of the generation system was limited to +/-10 V, and transmitted to the transducer via an attenuator and amplifier. The gain on the amplifier was selectable, allowing to adjust the acoustic level. A 13 dB attenuation was producing a maximum source level of 190 dB *re* 1μPa @ 1 m in the 10 to 20 kHz band. The emission was triggered with a GPS pulse per second for synchronization. The amplifier had two channels, so that it was possible to connect the generation system from HLS or UALG to the NURC transducers. The same deviation of the sampling frequency relative to the nominal frequency as the UALG system was found on the NURC generation system, so that a 96000 Hz sample frequency was in fact 96153 Hz (see above).

3.1.3 The HLS signal generation system

The PreSonus Firebox is an outboard 6-channel ADC and 2-channel DAC system that can record or play back digital time series to/from a host Windows or Mac computer.

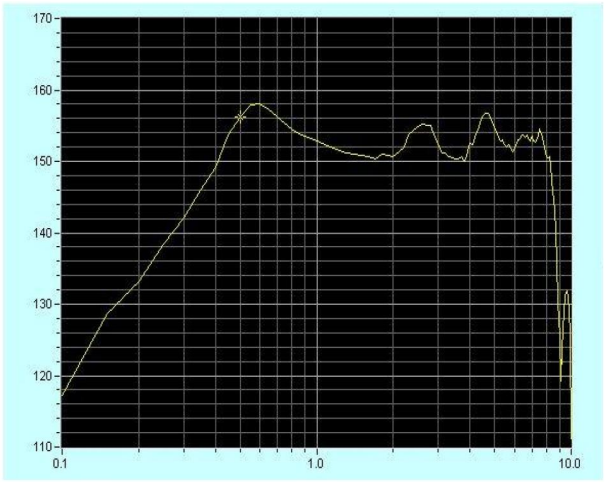

Figure 3.1: Transmit voltage response for the low frequency Lubell 1424HP acoustic projector.

The Firebox interfaces to the host computer using a Firewire interface. The Firebox can sample data at a number of standard sampling rates, including 44.1, 48, 96 and 192 kHz. It can sample or playback data having a dynamic range of 16 or 24 bits. A sample rate of 96 kHz was used for transmitting MF and HF waveforms, usually playing both bands through the left and right stereo channels provided by the Firebox. This capability to play two channels of digital waveforms simultaneously enabled transmission in all three bands throughout most of the experiment. A sample rate of 48 kHz was used for the LF band. In all cases, a dynamic range of 16 bits was used. Adobe Audition, a Windows digital sound editing application, was used to playback digital waveform files for transmission. The limitations of the PreSonus Firebox were:

- it could not be synchronized to a GPS clock;
- it was not set up to easily log its settings, especially its amplitude settings.

3.2 Acoustic sources

Acoustic signals were emitted from three sound sources in order to allow the different experiments enumerated in table 2.2 to take place - simultaneously or not. The acoustic band of emitted signals was roughly from 0.5 to 15 kHz, and was divided into three intervals: low frequency (LF) - 0.5 to 4 kHz; medium frequency (MF) - 4 to 8 kHz; and high frequency (HF) 8 to 15 kHz.

The UALG team made available a Lubell 1424HP for the network tomography and underwater communication experiments. This acoustic projector has useful emission band in the interval 500 to 8000 Hz (see figure 3.1). The NURC team made available two acoustic projectors mounted on a single frame, an ITC1007 with a resonance frequency of 11.5 kHz and an omnidirectional beam response in the 9 to 20 kHz interval, and a Neptune T170 with a beam response in the 4 to 9 kHz interval, both for the underwater communications and high frequency tomography experiments (see figure 3.2).

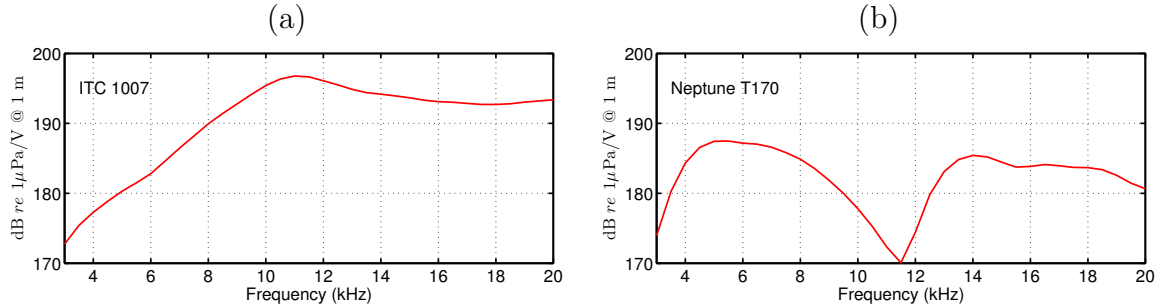

Figure 3.2: Transmit voltage response for the high frequency ITC-1007 acoustic projector (a) and the medium frequency Neptune T170 acoustic projector (b).

3.3 Emitted signals

There was a variety of signals transmitted during the experiment. Thanks to the number of acoustic sources and their wide transmitting band, all teams could transmit simultaneously their waveforms. Different waveforms transmitted with the same source were frequency and time multiplexed.

3.3.1 Low frequency tomography sequence

The UALG team designed a sequence of frames containing multi-tones (MT) or LFM chirps in two different frequency bands. The transmitted sequence has the following combination:

	Frame 1			Frame 2			Frame 3			Frame 4		
	P_{lu}	MT	blk	P_{ld}	LFM	blk	P_{hu}	MT	blk	P_{hd}	LFM	blk
Start f.(kHz)	1.1	0.5	-	1.6	0.5	-	1.5	1.8	-	4.0	1.8	-
Stop f.(kHz)	1.6	1.0	-	1.1	1.1	-	4.0	3.6	-	1.5	3.6	-
Duration (s)	1	48	2	1	1	2	1	48	2	1	0.5	1
Repetition	1×	1×	1×	1×	48 ×	1×	1×	1×	1×	1×	50×	1×

The total sequence consists of 4 frames, where each frame is a sequence consisting of a detection probe, a wavefom, and a blank interval. The detection probes were included in order to automatically detect the beginning of the respective frame by means of a correlation of the received probe with the emitted probe signal. These probes are LFM chirps, and their frequency bands are chosen such that probes and waveforms have no overlapping frequencies. In the first row of the diagram, P stands for *probe*, and the subscripts denote *low* or *high* band, and *upsweep* or *downsweep*. An upspeep LFM has a very low correlation with its downsweep counterpart, although the frequency band is exactly the same. The first and second frames begin with 1 s LFM chirps with 1.1 to 1.6 kHz frequency band. The probe in frame 3 consists of a concatenation of two 0.5 s upsweep LFM chirps, one from 1.5 kHz to 1.8 kHz, and the other from 3.6 kHz to 4.0 kHz. The idea was to make use of the available *holes* to maximize the bandwidth of the probe. Concerning the waveforms, the MTs consist of a superposition of sinusoids with frequencies 500, 550, 600, 650, 700, 750, 800, 900, and 1000 Hz, in the first frame, and 1800, 1900, 2100, 2300, 2600, 3000, and 3600 Hz, in the third frame. The first frame

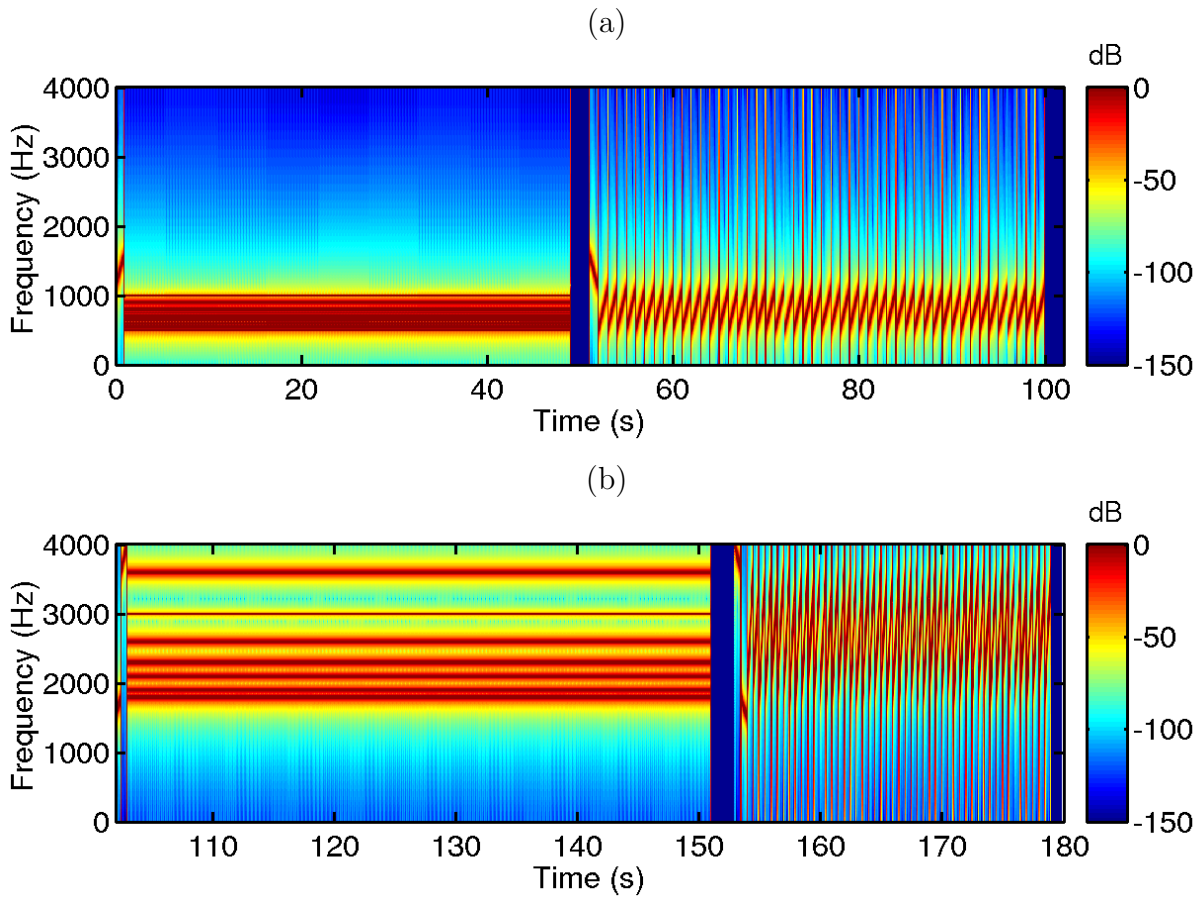

Figure 3.3: Spectrograms of the sequence emitted for the network tomograpgy experiments: first and second frames (a); third and fourth frames (b).

was designed for online inversions. The waveforms in the second and fourth frames are a repetition of LFM chirps with frequencies, lengths, and repetitions indicated in the diagram. Figure 3.3 shows spectrograms of the emitted sequence, first and second frames in (a), and third and fourth frames in (b). The blank intervals (blue) indicate the end of each frame.

3.3.2 The UAlg communications sequence

The UALG communications sequence has been composed in the following manner:

	p_{LFM}	blank	data	blank
Duration (s)	0.1	0.2	1	5
Repetition	50×		100×	1×

The sequence begins with a repetition of 50 LFM chirps denoted as p_{LFM}, with a duration of 100 ms and a silence of 200 ms in between, completing a total time of 15 s. The data consists of randomly generated symbols, with binary phase shift keying modulation, and a fourth-toot raised cosine pulse shape with a roll-off of 50%. The duration of the data

is 1 s, which is repeated 100 times. This sequence was composed for the mid-frequency (MF) and high-frequency (HF) bands. For the MF band the data has a bandwith of 1.5 kHz centered at 6250 Hz, the data is composed of 1000 symbols, and p_{LFM} has a starting-stop frequency from 5000 to 7500 Hz. For the HF band the data has a bandwith of 3 kHz centered at 12500 Hz, the data is composed of 2000 symbols, and p_{LFM} has a starting-stop frequency from 10 to 15 kHz.

3.3.3 The HLS waveforms for underwater communication

This section describes the various waveforms designed by the HLS Research team for underwater communications, and provides parameters used for their construction, specialized for each of the three bands. Due to the large number of signals of several modulation types and variations in their characteristics, this section provides only high-level descriptions of ths HLS waveforms and the waveform transmission lineups composed during the experiment. Detailed composition of the transmission lineups are provided in Appendix A of this report. Also listings of computer files and MATLAB® *m-file* descriptions that generated the HLS waveforms are given in Appendix B and Appendix C of this report.

Initially, the 500-4500 Hz band was transmitted through the LF source. Unfortunately, this was an oversight, since it interfered with the 4000-8000 Hz MF band. Therefore, some of the early transmissions will have slightly overlapped LF and MF bands. After this oversight was discovered, all LF waveforms were modified to use the 500-3500 Hz band. Note that the MF transmitted waveforms were not changed, only the LF waveforms.

LFM chirps

The LFM chirps are all 100 ms long, but were slightly expanded in time and frequency beyond the nominal 500-4500 (and later 500-3500 Hz) in the LF band, 4-8 kHz in the MF band, and 9-15 kHz in the HF band. This enabled a short ramp in amplitude to be added, in order to minimize the transient on the transducers and hopefully minimize leaking into adjacent bands. The taper at the start and end of the chirps was constructed by convolving a square window with a Hanning window.

Tone combinations

The tone combinations consisted of sets of frequency offsets from one another by 501 Hz (e.g. 1001, 1502, 2003, 2504, ...). The phases for the tones were randomized (uniformly distributed over 2π). The amplitudes were all equal. The pattern in frequencies and phases were intended to reduce the chances of getting a high peak-to-average-power ratio that is so common when multiple tones are added together (this is a well-known problem in communications systems that use multiple carriers, such as in OFDM).

PSK and M-sequences

M-sequences with $m = 11$ contain 2047 bi-polar symbols (1s and -1s). These bi-polar symbols are modulated using a BPSK modulation, for which the parameters are a symbol rate, an excess bandwidth for the shaping filter, and an excess bandwidth for a band

isolation filter. In all cases, we used a square-root raised cosine shaping filter with an excess bandwidth of 20%. We used a variety of symbol rates, depending on the band (4.8 kHz in the HF band, 3 kHz in the MF band, and 3 and 2 kHz in the LF band). To insure band isolation between the three bands, whenever a PSK-modulated waveform was transmitted, an additional filter with a sharper cutoff than the square root raised cosine shaping filter was applied to the waveforms. Let R_s be the symbol rate (4800 Hz for HF, and 3000 Hz for MF and LF). In all bands, R_s was selected so that even after the excess bandwidth used by the shaping filter (20% in all three bands), there would be some additional bandwidth that still fit into each of the respective LF, MF and HF bands. Thus, in the 9-15 kHz HF band, $R_s = 4800$, center frequency f_c=12 kHz, and the shaping filter used an extra 20% beyond that - 1.2×4800 or 5760 Hz, thus leaving some room ((6000-5760)/4800 or 5%) in the nominal 6000 Hz band for an additional, more powerful filter, to make sure the sidelobes of the shaping filter did not leak into the adjacent bands. Both the Lubell and the mid-frequency or MF source use a 4 kHz band, the Lubell using 500-4500 Hz, and the MF source using 4-8 kHz. Note that the Lubell and MF source bands overlap. Unfortunately, we transmitted LF and MF bands that overlapped by the same 500 Hz. We noticed this oversight after the first few test runs (need to check data for precise times), and corrected the various LF waveforms, keeping the MF waveforms the same. Thus, in most of the LF waveforms, there is a version that was used prior to finding out the overlap in bands. The m-sequences for the Lubell (LF) and MF sources use symbol rates R_s of 3000 symbols/s, center frequencies of 2500 and 6000 Hz, respectively, and roughly the same excess bandwidth parameters as the HF source. After we noticed the overlap in LF and MF bands, we modified the LF PSK parameters to use $B = 3000$, $R_s = 2000$, and $f_c = 2500$ Hz. In all cases, the square-root raised cosine *excess bandwidth* or alpha was 20%, and in all cases, we applied an additional band isolation filter using the remaining bandwidth beyond the $(1 + \alpha) \times R_s$ band, which was always smaller than the nominal total bands used (i.e. 500-4000 Hz for LF, 4000-8000 Hz for MF and 9-15 kHz for HF). M-sequences have a particular auto-correlation property that results in their being excellent probe pulses, but this property can only be realized in a multipath environment if the channel spread is covered by multiple M-sequences, concatenated head-to-tail. Thus, the present m-sequences have no gaps.

PRN sequences

The PRN waveforms were created using `rand`, the MATLAB® uniformly distributed random number generator. The raw PRN sequence was translated so that it had zero mean, and low-pass filtered using a filter designed to have a pass band that was the same as the symbol band for the comparable M-sequences, and a stop band at the edge of the total band allocated for each source. After constructing the PRN waveform at baseband, the waveform was bandshifted up to the center frequency used for each of the three sources (Lubell - 2500 Hz, MF - 6 kHz, HF - 12 kHz). In all cases, the raw random number sequences were saved to a MATLAB® MAT file.

3.3.4 The NURC tomography sequence

The signal designed for the high-frequency tomography phase, transmitted from the ship to the acoustic reception systems, are a succession of 4 signal types that have the same bandwidth-time product. The aim of these common feature is to compare, across a fairly long period of time corresponding to one tidal cycle, the stability of the propagation for several bandwidths, signal durations and central frequencies for the same amount of

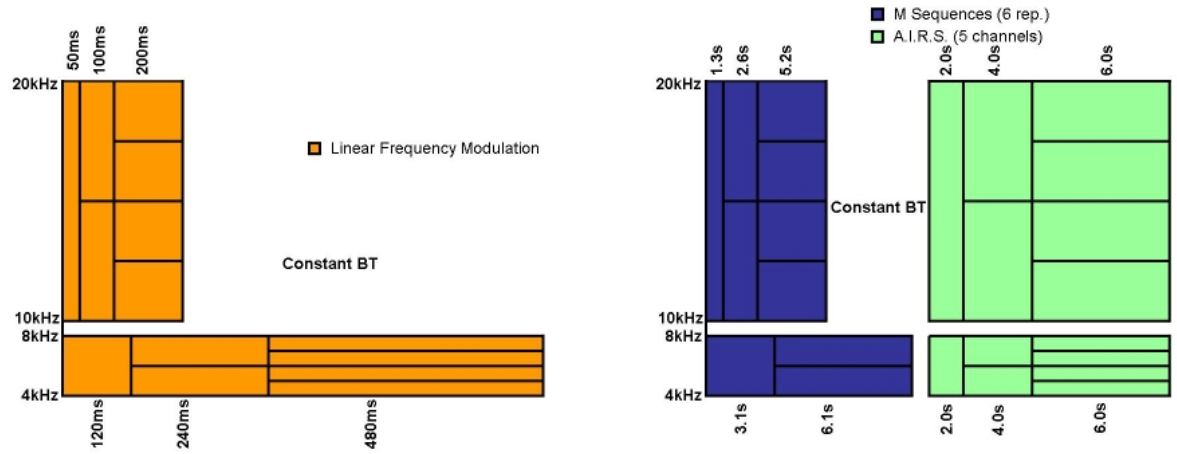

Figure 3.4: Schematic illustrating of the NURC signal sequence

Signal	Duration (s)	replica duration (ms)	replica start (s)
LFM	15.00	50.00	0.00, 1.50, 3.30, 5.10, 7.50, 9.90, 12.30
M-seq	29.00	214.06	15.00, 16.50, 19.30, 22.10, 27.50, 32.90, 38.30
AIRS	44.00	2000.00	44.00, 46.20, 50.40, 54.60, 62.80, 71.00, 79.20
CWS	10.80	-	88.00

Table 3.2: Description of the high-frequency NURC sequence in terms of signal type duration, replica duration, number of replicas, and starting time of each replica.

energy produced. The 4 types of signals are:

- linear frequency modulations;
- m-sequences;
- adaptive instant record signals (AIRS);
- continuous sine waves (CWS);

each type of signal is always repeated 6 times, and separated by 200ms of silence, which allows summation and average. The signal band is 9.6 to 19.6 kHz, and the sampling rate at the signal generation is 96000 samples per second. Figures 3.4 illustrates the principle behind the design of this sequence. Tables 3.2 and 3.4 describe the duration and replica start times of each signal type in the sequence respectively for high and medium frequency intervals, and tables 3.3 and 3.5 describe the replicas in terms of spectral features such as central frequency, bandwidth, and minimum and maximum frequencies, respectively for high and medium frequency intervals.

3.3.5 Waveform transmission lineups

This section describes the lineups of waveforms during the High-Frequency Tomography phase on July 12 (Julian Day 193), Probes and Communications phase on Friday, July

Replica #	f_c (kHz)	T (ms)	B (kHz)	$f_{\min}$ (kHz)	$f_{\max}$ (kHz)
1	14.8	50	9.6	10.0	19.6
2	12.4	100	4.8	10.0	14.8
3	17.2	100	4.8	14.8	19.6
4	11.2	200	2.4	10.0	12.4
5	13.6	200	2.4	12.4	14.8
6	16.0	200	2.4	14.8	17.2
7	18.4	200	2.4	17.2	19.6

Table 3.3: Description of the high-frequency NURC sequence in terms of central frequency, duration, bandwidth, minimum and maximum frequencies of each replica.

Signal	Duration (s)	replica duration (ms)	replica start (s)
LFM	24.00	120.00	0.00, 1.92, 4.56, 7.20, 11.28, 15.36, 19.44
M-seq	17.00	513.75	24.00, 27.30, 33.70
AIRS	44.00	2000.00	41.00, 43.20, 47.40, 51.60, 59.80, 68.00, 76.20
CWS	10.80	-	85.00

Table 3.4: Description of the medium-frequnncy NURC sequence in terms of signal type duration, replica duration, number of replicas, and starting time of each replica.

Replica #	f_c (kHz)	T (ms)	B (kHz)	$f_{\min}$ (kHz)	$f_{\max}$ (kHz)
1	6.0	120	9.6	1.2	10.8
2	3.6	240	4.8	1.2	6.0
3	8.4	240	4.8	6.0	10.8
4	2.4	480	2.4	1.2	3.6
5	4.8	480	2.4	3.6	6.0
6	7.2	480	2.4	6.0	8.4

Table 3.5: Description of the medium-frequency NURC sequence in terms of central frequency, duration, bandwidth, minimum and maximum frequencies of each replica.

13 (Julian Day 194), and the Networked Tomography phase on Saturday, July 14 (Julian Day 195).

Each row of the tables 3.6 to 3.10 represents one minute of transmitted data. The tables show a complete cycle, which was repeated over substantial intervals (tens of minutes to tens of hours).

Two different cycles are shown below for the Probes/Comms phase, a *deep* cycle for runs where the HF and MF sources were towed deep (60 m), and a *shallow* cycle for runs where the HF and MF projectors were towed at a shallow depth (14 m). The Lubell was limited to shallow depths.

The reason for deploying the MF/HF source assembly at two different depths was to collect data for comparing the channel impulse response function in low and high frequency bands. The Lubell 1424 HP low frequency source could only be towed at a depth of 10 m, so the only way to get low and high frequency measurements at the same depth was to also tow the MF/HF sources at a shallow depth.

However, collecting data for acoustic communications was another goal of this phase, and it is well known that acoustic communications are more difficult when the source or receiver is deployed at a shallow depth, usually because the multipath structure is more stable and focused at greater depths. As a result, we also wanted to collect data with the MF and HF sources deep, which is a better depth for acoustic communications. This is the reason for using two source depths. Slightly different lineups of waveforms were used during these two configurations.

Lineup for waveform transmitted in LF band during High-Frequency Tomography

The LF waveform used in this phase was transmitted from the Firebox and consisted of three minutes of the Networked Tomography probe waveforms (3 minutes long) provided by Cristiano Soares (U. of Algarve) and the target-lf waveform from HLS Research (6 minutes long) for field-calibration. While this LF waveform was being transmitted at a rate of once every 9 minutes, the U. of Algarve and NURC playback systems transmitted waveforms provided by NURC (described in section 3.3.4). Table 3.6 describes the 18-minute cycle that was transmitted during the High-Frequency Tomography phase of the experiment. From now on this lineup is referred as *HF tomo*.

Lineup for Probes and Communications deep transmissions

Table 3.7 shows the timeline of the 15-minute cycle that was transmitted during the Probes and Comms phase of the experiment when the MF/HF sources were deep. See Appendix B for a detailed breakdown of the files that were combined and sequenced together to form that sequence. From now on this lineup will be referred as *P&C deep*.

Lineup for Probes and communications shallow transmissions

Table 3.8 shows the lineup of the 15-minute cycle that was transmitted during the Probes and Comms phase of the experiment when the MF/HF sources were shallow. See Ap-

Start (minutes)	LF	MF	HF
0	UAlg tomo	NURC-MF	NURC-HF
1	UAlg tomo	NURC-MF	NURC-HF
2	UAlg tomo	NURC-MF	NURC-HF
3	HLS target-LF	NURC-MF	NURC-HF
4	HLS target-LF	NURC-MF	NURC-HF
5	HLS target-LF	NURC-MF	NURC-HF
6	HLS target-LF	NURC-MF	NURC-HF
7	HLS target-LF	NURC-MF	NURC-HF
8	HLS target-LF	NURC-MF	NURC-HF
9	UAlg tomo	NURC-MF	NURC-HF
10	UAlg tomo	NURC-MF	NURC-HF
11	UAlg tomo	NURC-MF	NURC-HF
12	HLS target-LF	NURC-MF	NURC-HF
13	HLS target-LF	NURC-MF	NURC-HF
14	HLS target-LF	NURC-MF	NURC-HF
15	HLS target-LF	NURC-MF	NURC-HF
16	HLS target-LF	NURC-MF	NURC-HF
17	HLS target-LF	NURC-MF	NURC-HF

Table 3.6: Lineups in three frequency bands during the High-Tomography phase on Julian day 193 - HF tomo.

Start (minutes)	MF	HF
0	UAlg PSK	UAlg PSK
1	UAlg PSK	UAlg PSK
2	UAlg PSK	UAlg PSK
3	UAlg PSK	UAlg PSK
4	UAlg PSK	UAlg PSK
5	UAlg PSK	UAlg PSK
6	UAlg PSK	UAlg PSK
7	UAlg PSK	UAlg PSK
8	NURC LFM McCoy	NURC LFM McCoy
9	HLS target-mf	HLS HF-PSK
10	HLS target-mf	HLS HF-OFDM
11	HLS target-mf	HLS HF-FSK1
12	HLS target-mf	HLS HF-FSK2
13	HLS target-mf	HLS HF-probes
14	HLS target-mf	HLS HF-probes

Table 3.7: Probes and communications lineup for deep source transmissions - P&C deep.

Start (minutes)	MF	HF
0	UAlg PSK	UAlg PSK
1	UAlg PSK	UAlg PSK
2	UAlg PSK	UAlg PSK
3	UAlg PSK	UAlg PSK
4	UAlg PSK	UAlg PSK
5	UAlg PSK	UAlg PSK
6	UAlg PSK	UAlg PSK
7	UAlg PSK	UAlg PSK
8	NURC LFM McCoy	NURC LFM McCoy
9	HLS lfm-mf	HLS HF-PSK
10	HLS mseq-mf	HLS HLS-OFDM
11	HLS lfm-mf	HLS HLS-FSK1
12	HLS mseq-mf	HLS HF-FSK2
13	HLS lfm-mf	HLS HF-PSK
14	HLS mseq-mf	HLS HF-OFDM

Table 3.8: Probes and communications lineup for shallow source transmissions - P&C shallow.

Start (minutes)	LF
0	UAlg tomo
1	UAlg tomo
2	UAlg tomo
3	HLS target-lf2
4	HLS target-lf2
5	HLS target-lf2
6	HLS target-lf2
7	HLS target-lf2
8	HLS target-lf2
9	blank

Table 3.9: Lineup for the LF transmitter - LF tomo.

pendix B for a detailed breakdown of the files combined and sequenced to form that timeline. From now on this lineup will be referred as *P&C shallow*.

Lineup for low-frequency tomography and field calibration

Table 3.9 presents the 10 minute cycle that includes the UAlg tomography sequence and the HLS Research field calibration sequence. These signals were transmitted using the Lubell 1424HP low frequency projector. This sequence was transmitted both during the deep and shallow deployments of the MF/HF sources. From now on this lineup will be referred as *LF tomo*.

Start (minutes)	LF	MF	HF
0	UAlg tomo	NURC LFM McCoy	LFM McCoy
1	UAlg tomo	HLS lfm-mf	UAlg PSK
2	UAlg tomo	HLS mseq-mf	UAlg PSK
3	HLS target-lf2	HLS lfm-mf	UAlg PSK
4	HLS target-lf2	HLS mseq-mf	UAlg PSK
5	HLS target-lf2	HLS lfm-mf	UAlg PSK
6	HLS target-lf2	HLS mseq-mf	UAlg PSK
7	HLS target-lf2	HLS lfm-mf	UAlg PSK
8	HLS target-lf2	HLS mseq-mf	UAlg PSK
9	UAlg tomo	NURC LFM McCoy	NURC LFM McCoy
10	UAlg tomo	UAlg PSK	HLS HLS-PSK
11	UAlg tomo	UAlg PSK	HLS HLS-OFDM
12	HLS target-lf2	UAlg PSK	HLS HLS-FSK1
13	HLS target-lf2	UAlg PSK	HLS HLS-FSK2
14	HLS target-lf2	UAlg PSK	HLS HLS-PSK
15	HLS target-lf2	UAlg PSK	HLS HLS-OFDM
16	HLS target-lf2	UAlg PSK	HLS HLS-PSK
17	HLS target-lf2	UAlg PSK	HLS HLS-OFDM

Table 3.10: Network tomography lineup - Networked tomo.

Lineup for Networked tomography transmissions

Finally, table 3.10 describes the 18-minute cycle that was transmitted during the Networked Tomography experiment. The LF waveforms were played through the UAlg system. The MF and HF were played through the PreSonus Firebox system. See Appendix B for a more detailed breakdown of the files combined and sequenced to form the timeline of events shown in Table 3.10. From now on this lineup will be referred as *Networked tomo*.

3.4 The Acoustic Oceanographic Buoy - version 2 (AOB2)

The AOB concept started in 2002, during the LOCAPASS project[1], where a preliminary version of the AOB was developed (see AOB1 report [18]) for more details). That first version of the AOB, AOB1, was tested during the Maritime Rapid Environmental Assessment (MREA) sea trials in 2003 off the Italian coast, north of Elba I. [3] and in 2004 off the portuguese coast, approximately 50 km south from Lisbon [12]. The

AOB2 hardware and software system is described in [2], while here only a brief description is made, in relation with the necessary characteristics for data processing.

During the MREA/BP'07 sea trial two AOBs version 2 were used. Appart from small

[1]Passive source localization with a random network of acoustic buoys in shallow water (LOCAPASS), funded by the Foundation of Portuguese Universities and the Ministery of Defence.

details such as float type, colour and so on, the two buoys are exactly the same in all respects but the sensor array. A detailed sensor array description is given below in section 3.4.2.

3.4.1 AOB2 generics

The AOB2 is a light acoustic receiving device that incorporates last generation technology for acquiring, storing and processing acoustic and non-acoustic signals received in various channels along a vertical line array. The physical characteristics of the AOB2, in terms of size, weight and autonomy, will tend to those of a standard sonobuoy with, however, the capability of local data storage, processing and online data transmission. Data transmission is ensured by seamless integration into a wireless lan network, which allows for network tomography within ranges up to 10/20 kms. In this second AOB prototype several capabilities were improved relative to the first system tested in 2003/04, namely the buoy container and electronics / data acquisition. The container now has the dimensions and weight of a standard sonobuoy. Electronics and batteries are housed in two separate containers: the battery container houses a high performance Li-ion 15V / 48Ah, capable of driving the AOB2 during more than 12 hours and weighting only 4.5 Kg; the electronics container receives a PC104+ stack with both comercial off the shelf (COTS) boards and proprietary boards specifically designed for the AOB2. The electronics stack also has a OEM GPS and a wlan amplifier for communications with the base station. The details of the electronic and mechanic parts are given in [19], while a brief description of the receiving arrays and data acquisition systems are given in the next two sections.

3.4.2 AOB2 receiving array

The main differences between the two AOBs are in the sensor arrays since one array has 8 hydrophones and the other has got 16 hydrophones, so the two buoys will be therefore called as AOB21 (8 hydrophones) and AOB22 (16 hydrophones), respectively. The two hydrophone arrays share the fact that they are light systems composed of dedicated balanced twisted pairs for each hydrophone and a common power line attached to a 5 mm kevlar rope enveloped in a air fairing sleeve to maintain all wires together (see figure 3.5(a)). This system has a reduced water drag and allows for easy field maintenance when and if necessary. The hydrophone spacing and depth for the two arrays when deployed at sea is shown in figure 3.5(b). The AOB21 array has 8 hydrophones oddly distributed in the 70 m total acoustic aperture, at depths of: 10, 15, 55, 60, 65, 70, 75 and 80 m. The ensemble hydrophone - pre-amplifier were manufactured by Sensor Technology (Canada). The hydrophone sensitivity is -193.5 $\pm$ 1 dBV re 1 μPa 20° C for both broadside and endfire up to 18 kHz and with a flat frequency response from 1 Hz up to 28 kHz. The pre-amplifier is a low noise differential amplifier that has a constant gain of 40 dB in the whole frequency band of interest between 10 Hz up to 50 kHz. Its noise has been measured to be smaller than 20 nV/$\sqrt{Hz}$. The AOB22 array has 16 hydrophones equally spaced at 4 m with the first hydrophone located at 5.5 m from the bottom of the buoy contained which corresponds to approximately 6.5 m from sea surface. The hydrophone is manufactured by Sensor Technology (Canada) and is the same model as that used in the AOB21. The pre-amplifier is a low noise differential amplifier that has a constant gain of 40 dB in the whole frequency band of interest between 10 Hz up to 50 kHz and is, in all respects, similar to that of the AOB21. As it will be seen during the deployments, the pre-amplifier gain was often insufficient to fullfil the analogue to digital converter (ADC)

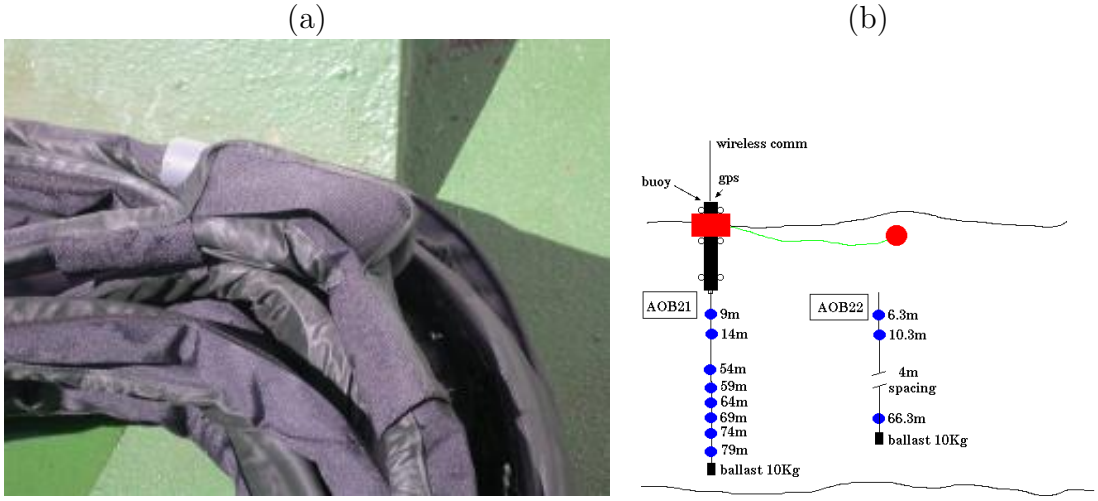

Figure 3.5: *Acoustic Oceanographic Buoy - version 2: receiving array hydrophone (a) and surface buoy structure (b).*

Year day	JD	AOB21	AOB22
Wed July 11	192	10:45 - +/-5V	10:39 - +/-2V
Wed July 11	192	13:10 - +/-2V	12:02 - +/-1V
Thu April 12	193	07:50 - +/-2V	07:25 - +/-1V
Fri April 13	194	09:46 - +/-2V	09:34 - +/-1V
Fri April 13	194	11:15 - +/-1V	-
Sat April 14	195	08:41 - +/-1V	08:35 - +/-1V

Table 3.11: *AOBs gain changes during sea trial. Times are in GMT.*

±5 V sensitivity at the frequencies used during the transmissions. This required some field tuning of the data acquisition in order to better use the dynamics of the ADC board.

3.5 AOB2 data acquisition

The data acquisition was performed by a dedicated ADC board attached to a DSP board. The ADC board itself is an LTC1864 from Linear Technology based on successive approximation with 16 bits, four modules and a total agregate frequency per module of 250kHz. The anti-aliasing filters are 8 pole low-pass analog Chebyshev implementations with a cutoff frequency of 16 kHz. As explained above due to the pre-amplifier constant low gain of 40 dB when working in the high frequency range of the bandwidth, it was necessary to change the ADC sensitivity according to the source - receiver distance. The ADC has an internal variable gain setting leading to input sensitivities of ±1, ±2, ±5 and ± 10 volts. Sensitivity changes made during this sea trial are shown in table of figure 3.11(a). The first entry of each day is the acquisition range at the moment of deployment.

3.6 Received signals

3.6.1 Data format

The AOB data, both acoustic and non acoustic, received on the AOB2 are stored on data files using a proprietary format that can be read using the m-file `ReadVLAData.m` shown in appendix D. This format can be summarized as follows:

- **an ASCII header:** cruise title, UTC GPS date and time of first sample on file, Lat - Lon GPS position, characteristics of non-acoustic and acoustic data such as sampling frequency, number of channels, sample size and total number of samples
- **non-acoustic data:** temperature data in binary format
- **acoustic data:** acoustic data in binary format

Each data file contains 24 s worth of data and there is no data loss between files. Data files are acquired in sequence with file names reflecting Julian day, hour, minutes and seconds with the extension ".vla". The time used in the file name is obtained from the computer clock so it should not be used for synchronization purposes and it may differ from the GPS time in the header. **The time stamp in the header of each file is the exact GPS - GMT time of the first acoustic sample in the file** and it can and should be used for synchronization and time of flight measurement purposes, if required. The sampling frequency used during RADAR'07 was 50000 samples per second. The Lat/Lon location written in the header is that given by the AOB2 GPS at the time of the first sample. A decimal degree notation was adopted in order to simplify its usage for calculation and plotting purposes (inside `MATLAB`®, for example).

3.6.2 Drift 1: Julian day 192

Day 192 was dedicated to test the different systems on board used during RADAR'07. This day permited testing the acoustic transmission sytems, the AOBs and SLIVA.

The AOBs AOB21 and AOB22 were respectively deployed at times 10:45 and 10:39 of Julian day 192. The UAlg and HLS Research teams transmitted waveforms according to the schedule shown in table 3.12. These sequences do not correspond to any of the lineup given in section 3.3.5. The UALG LF tomo sequence is described in section 3.3.1, and the HLS research waveforms consisted of LFMs, tones, and m-sequences are described in section 3.3.3.

The UALG LF tomography sequence started to be transmitted at 12:18:00 GPS UTC time with a repetition rate of 6 minutes, and ended at 13:57, using the UALG signal generation system. On the MF and the HF band the HLS Research team transmitted lfm-mf and lfm-hf sequences continuously using the NURC signal generator. Some final remarks are:

- It was noticed that the UALG sequence appears folded in the spectrograms of the received waveforms with central frequency 5 kHz, i.e. the energy at a frequency f_i appears at frequency $F_\mathrm{s} - f_i$. This folding effect was generated by the UALG signal generator, due to $F_\mathrm{s} = 10$ kHz.

Event	acoustic source		
	LF	MF	HF
Start HLS Research lfm-mf & lfm-hf		10:47	10:47
Stop HLS Research lfm-mf & lfm-hf		11:45	11:45
Start HLS Research lfm-mf & lfm-hf		11:45	11:45
Stop HLS Research lfm-mf & lfm-hf		12:15	12:15
Start HLS Research lfm-mf		12:16	
Start UALG LF tomo	12:18		
Stop HLS Research lfm-mf		12:31	
Start HLS Research lfm-mf		12:31	
Stop HLS Research lfm-mf		12:43	
Start HLS Research lfm-mf & lfm-hf		13:03	13:03
Stop UALG LF tomo	13:57		
Stop HLS Research lfm-mf & lfm-hf		14:20	14:20

Table 3.12: Transmission schedule during Julian day 192 at the 3 acoustic sources.

- The acoustic acquisition of AOB21 failed between times 12:13 and 12:40.
- During silence intervals or while acoustic emitter were shut off a waveform in the band 6 to 16 kHz with a repetition period of about 0.65 s was noticed on both AOBs and on every acoustic channel. So far, the source of this waveform could not be identified.

Figure 3.6 shows examples of signals received during Drift 1 in all three frequency bands. Figure 3.6(a) shows an interval of the NURC sequence received at receiver #4, where the LFM chirps and tones in both bands can be clearly distinguished. Figure 3.6(a) shows part of the UALG sequence, where the complete interval of multi-tones and the beginning of the LFM chirps interval can be observed, and the NURC LFM sequence in the MF and HF bands. All received waveforms have a clear outstanding from background noise.

3.6.3 Drift 2: Julian day 193

This day was mainly dedicated to HF tomography, as transmissions of waveforms in the MF and HF bands designed by the NURC team were transmitted during almost 24 hours, with the MF/HF source pair deployed at 70 m depth transmitting the *HF tomo* lineup (see table 3.6). The UALG and HLS research teams proceeded with the transmission of the low-frequency component of the *HF tomo* lineup using the LF acoustic source, aiming respectively at low frequency tomography and field calibaration, by time multiplexing their sequences in the same signal generator. Table 3.13 shows start and stop times for this day. The fact that starts and stops of the same sequence appears repeated reflects only the fact that that lineup is divided through different signal and transmission systems. Figure 3.7 shows an example of received signals emitted by the three teams. In the LF band it is possible to observe the LFM series of the end of the UALG sequence followed by the HLS research probes sequence with a clear outstanding from the background noise. In the MF and HF bands the NURC sequences are clearly visible. However, the received HF signals appear to be 20 dB above the MF signals. The effect of the anti-aliasng filter can be clearly seen as the energy above 16 kHz is significantly attenuated. (Note that the NURC signals with frequencies up to 20 kHz were designed for reception at the NURC's

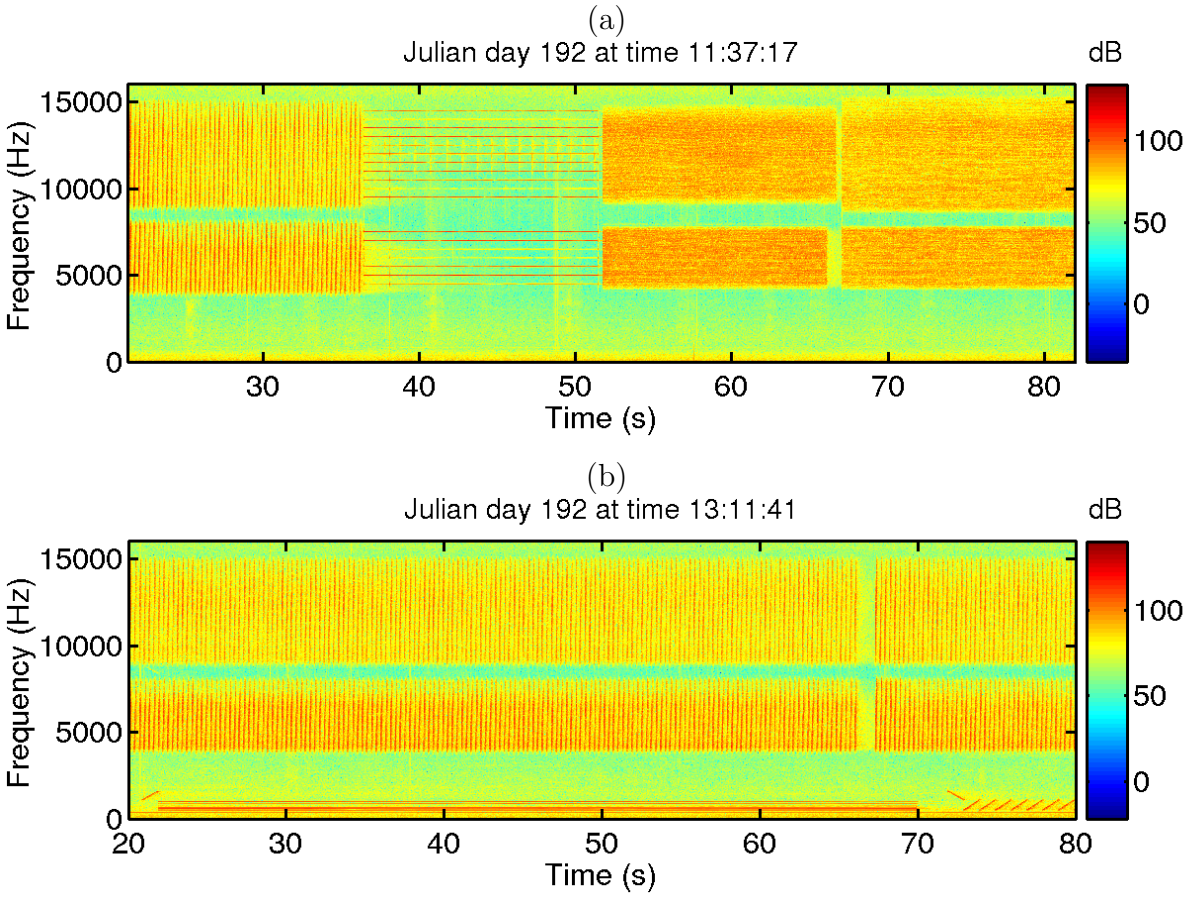

Figure 3.6: Spectrograms of signals received at receiver #4 of AOB22 during Drift 1: NURC signals received at approximately 2.4 km from the emitter (a); UALG LF and NURC HF tomography waveforms received at approximately 2.0 km from the emitter.

Event	acoustic source		
	LF	MF	HF
Start HF tomo		09:17	09:17
Start HF tomo	10:05		
Stop HF tomo	17:05		
Stop HF tomo		17:10	17:10

Table 3.13: Transmission schedule during Julian day 193 for the 3 acoustic sources.

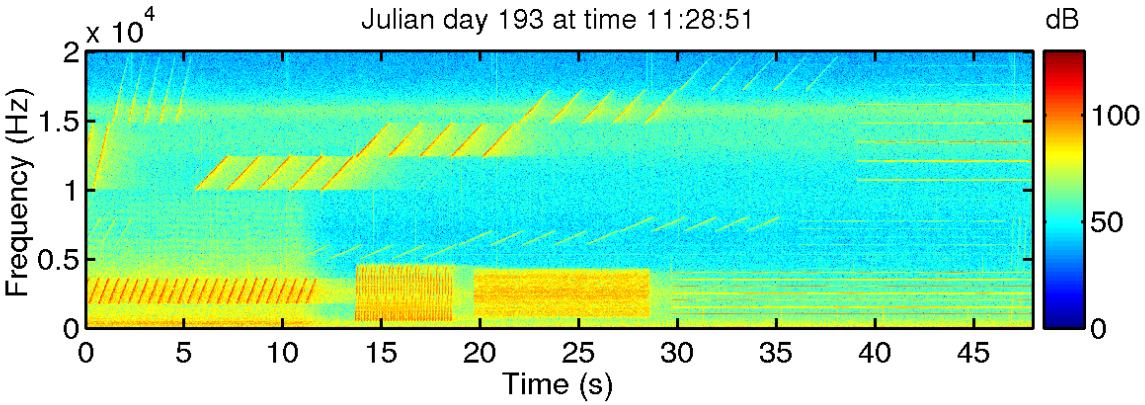

Figure 3.7: Spectrograms of signals received at receiver #4 of AOB22 during Drift 2 at approximately 1.7 km from the emitter.

receiving array SLIVA.) One final remark is that it was noticed that receiver 16 of AOB22 is very noisy during the whole drift, such that the respective data might be useless.

3.6.4 Drift 3: Julian day 194

This day was mainly dedicated to underwater communications, since the MF/HF source pair was used only to transmit UAlg/HLS Reasearch communication sequences. The MF/HF pair was deployed at different depths as summarized in table 2.3 at 60 m depth, but with ship movements it became as shallow as 40 m. The LF source transmitted the UAlg LF tomography and HLS field calibration signals. AOB21 and AOB22 were deployed at respective times 09:46 UTC and 09:34 UTC in free drifting configuration. The sequence for the LF acoustic source consisted of a time multiplex of UALG LF tomography sequence (3 minutes) and a HLS Research field calibration sequence (6 minutes). Initially, the repetition period was set to 9 minutes and the LF acoustic source started transmission at 10:31 UTC. However, a problem related to the coincidence in the sequence length and repetition period was detected immediately, and the signal generation was interrupted. Then, the repetition time was set to 10 minutes and transmission resumed at 10:56 and ended at 18:20 UTC. The HLS Research team transmitted their waveforms over three different time intervals as seen in table 3.14, by changing the depth of the MF/HF pair to 10 or 60 m, and respectively transmitting the lineups in tables 3.8 and 3.7. Figure 3.8 shows an example of signals received during Julian day 194.

Event	acoustic source		
	LF	MF	HF
Start P&C shallow		10:16	10:16
Start LF tomo	10:31		
Stop LF tomo	10:39		
Start LF tomo	10:56		
Stop P&C shallow		11:41	11:41
Start P&C deep		11:55	11:55
Stop P&C deep		15:42	15:42
Start P&C shallow		15:57	15:57
Stop LF tomo	18:20		
Stop P&C shallow		18:22	18:22

Table 3.14: Transmission schedule during Julian day 194 at the 3 acoustic sources.

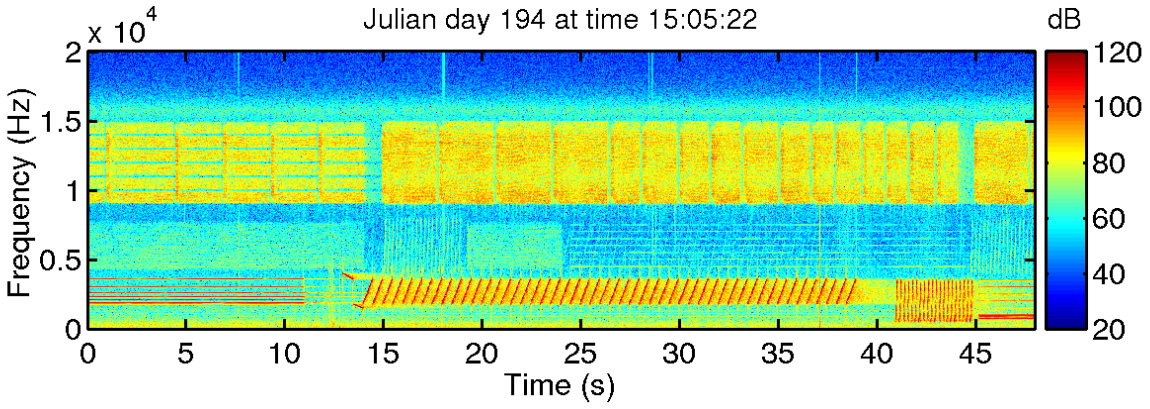

Figure 3.8: Spectrograms of signals received at receiver #4 of AOB22 during Drift 3 at approximately 1.4 km from the emitter.

Event	acoustic source		
	LF	MF	HF
Start P&C deep		09:00	09:00
Start P&C LF	09:19		
Stop P&C deep		11:07	11:07
Start Networked tomo		11:08	11:08
Stop P&C LF	17:19		
Stop Networked tomo		17:19	17:19

Table 3.15: Transmission schedule during Julian day 195 at the 3 acoustic sources.

	Stop	Resume
AOB21	08:43	09:19
AOB21	10:35	11:54
AOB21	13:29	14:22
AOB22	12:05	12:11

Table 3.16: Time intervals in which data acquisition was interrupted due to AOBs' malfunction.

3.6.5 Drift 4: Julian day 195

This day was mainly dedicated to network tomography. The HLS Research team transmitted the P&C deep sequence using the MF/HF pair at 60 m depth between 09:05 and 11:08 GMT. Then the emitted lineup was changed to the Networked Tomo sequence for the remaining time with the MF/HF pair at 60 m nominal depth until time 14:06 GMT (see table 2.3). The LF source was used to transmit the sequence containing the UAlg LF tomography and the HLS field calibration signals. The main particularity was the geometric setup, as the ship performed a trajectory with stations where the position was maintained constant during a certain time (see table 2.5). AOB21 was deployed at 08:41 UTC and AOB22 before 08:35 (precise time is unknown). Table 3.15 shows the transmission schedules during day 195. Several failures in AOB21 happened over the drift, causing the acquisition to be interrupted. Table 3.16 shows at which times the AOBs stopped and resumed acquisition due to technical failure.

Figure 3.9 shows an example of signals received during Julian day 195.

3.7 Channel variability

A common preliminary processing consists in matched filtering the incoming data with the emitted signal so as to obtain an estimate of the channel acoustic impulse response. This processing, also known as time-compression, gives a channel response estimate that is as good as the frequency band of the emitted signal is large and the arrival times are resolvable. The obtained matched-filter output is known as the arrival pattern estimate. Of course the channel response (or arrival pattern) varies in time according to the medium variability and in space according to the experiment geometry. During RADAR'07 either the receiving array or both the emitting source and the receiving array were moving along time - so time and space variability effects are mixed in the estimated channel response and can only be separated by introducing *a priori* knowledge of the system geometry

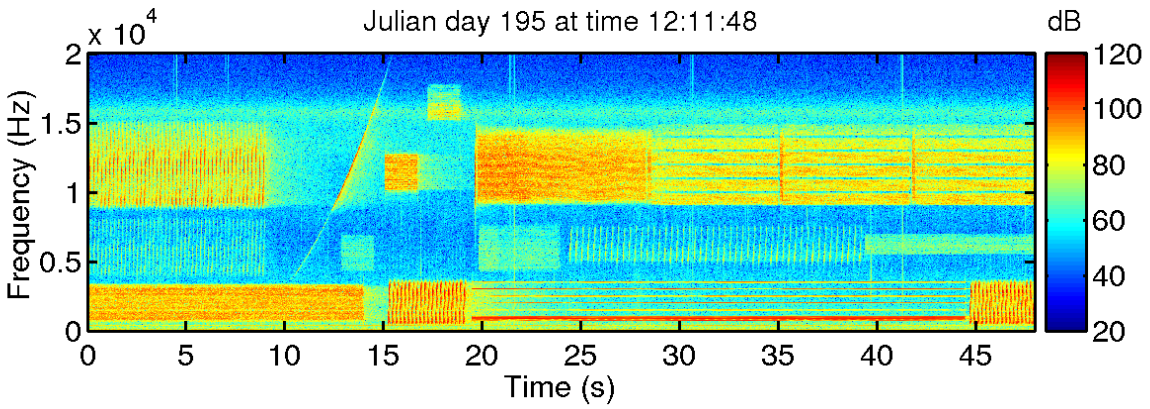

Figure 3.9: Spectrograms of signals received at receiver #4 of AOB22 during Drift 4 at approximately 1.7 km from the emitter.

or appropriate simultaneous space-time processing. In this preliminary assessment it is important to assert of the channel variability both along the sensor array (which to some extent defines the diversity of the received field) and along time. If the spatial aperture of the array is more or less fixed and does not oscillate with time, the same does not holds for the channel geometry, therefore it is important to define what is meant by channel variability along time. There is a short time variability, on the scale of a digital communications message - a few seconds -, and there is a larger term variability on the scale 15 minutes up to the hour or so, which is an environmental-induced variability.

In order to illustrate the short scale variability induced by small motion and environmental variability the sequence received at time 13:11 GMT of Julian day 192 on hydrophone 4 of AOB21 was pulse compressed. This sequence represents an observation window of 46 s (see Figure 3.6(b)), and was chosen for the very low variability in range between emitter and receiver at this time (see figure 2.15). The relatively high repetition rate of the LFM sequence emitted at this time (one chirp every 0.3 s), both in the medium and high frequency bands, allows to estimate the channel response at a very high rate.

Figure 3.10 shows the envelope of the pulse compression of the received sequence being considered. The correlation amplitude varies smoothly and almost periodically, which appears to be a fading effect of the channel. This might be related to receiver motion and the interaction with scatterers that may cause close arrivals to sum up more or less constructively according to the small variability of arrival times and phases. The interaction of the acoustic field with scatterers, such as the ocean surface and seafloor, or even the watercolumn itself, becomes more and more significant as the waveform frequency is increased.

Figure 3.11 shows the time aligned arrival patters obtained by pulse compression of the received data. The arrival structure is very stable during this interval.

Figure 3.12 shows the estimated average correlation peak of the pulse compression with a given time apart over the window for the medium frequency and HF bands. The idea is to measure the degree of decorrelation after a given. Here it is given as the average of the maximum of

$$r(\tau;\Delta t) = \int_{-T}^{T} \hat{h}(t) * \hat{h}[-(t+\Delta t)+\tau]dt \tag{3.1}$$

over the observation window for different Δt. Time T is the length of $\hat{h}(t)$. Note that $\hat{h}(t) = y(t) * s(-t)$, where $y(t)$ is the received and $s(t)$ is the emitted signal. It is seen

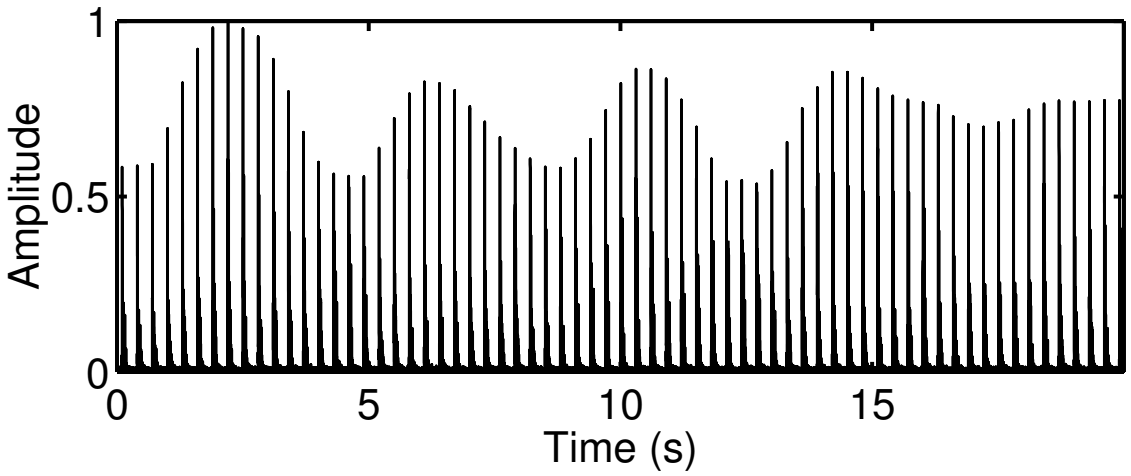

Figure 3.10: Envelope of the pulse compressed LFM chirps in the band 4000 to 8000 Hz.

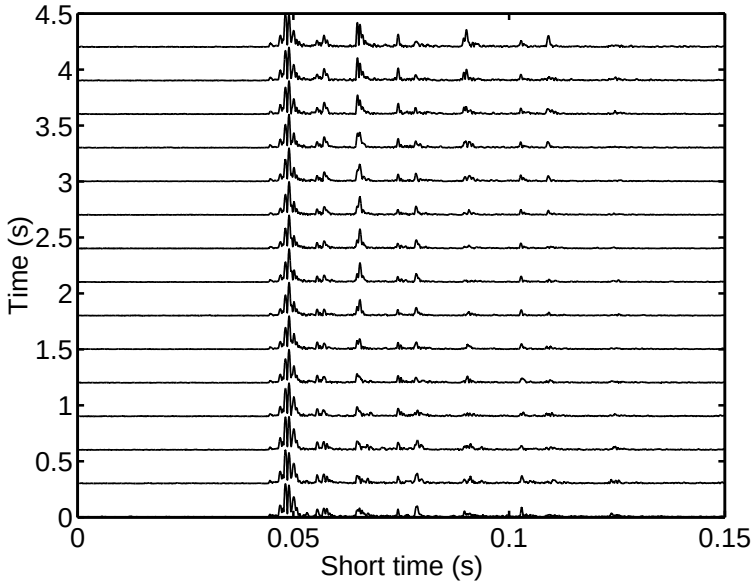

Figure 3.11: Aligned envelopes of the pulse compressed LFM chirps in the band 4000 to 8000 Hz.

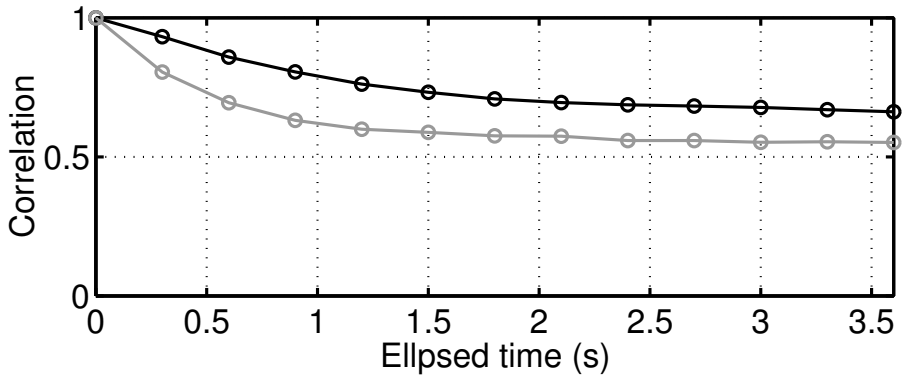

Figure 3.12: Correlation time of pulse compressed LFM chirps in the band 4000 to 8000 Hz: MF band in black; HF band in gray.

that, as expected, the *fall off* of the correlation is significantly faster in the HF band than in the MF band. In the HF band the average correlation is about 0.56 after only 2.5 s. Although the arrival structure is very stable, the correlation of the full field rapidly falls off with time due to the weak stability of the phases. This might be an important issue for coherent processing algorithms.

Chapter 4

Online matched-field tomography

One of the objectives of the RADAR project is to test the possibility of acoustically assessing the oceanic environment by means of a network of free-drifting acoustic receiving systems. This objective is part of a broader frame that is Acoustic Rapid Environmental Assessment (REA), where one of the questions is whether acoustics can give a contribution to REA. In an operational context it is necessary to have acoustic versatile instrumentation available. For example, it is necessary to have acoustic receiver devices with features such as self-locatable in terms of earth coordinates and capable to communicate at high data rates.

From the practical point of view SiPLAB has since 2002 invested a significant effort in tailoring the acoustic hardware with these features, by constructing AOBs with a GPS receiving and wireless communication systems, on one hand, and the development of an operational inversion software on the other hand. The idea is to run the inversion software in a processing platform on board of the research vessel, and download the data collected and stored at the AOBs at any time during deployments for immediate inversion.

During the RADAR'07 an operational processing platform has been set up on board of NRP D. Carlos I. Figure 4.1 shows a simplified scheme of that network. Note that the AOBs are part of that network since they have also a defined Internet Protocol (IP) number and are accessed the same way as any other computer node in the remaining network. This computer network integrated a data server, two dual processor processing nodes, laptops used as workstations, and the two AOBs, all communicating through standard network protocols such as the File Transfer Protocol (FTP), Secure Shell (SSH), or others.

4.1 The inversion software

Over the years an acoustic inversion software capable of compiling all necessary input data such as watercolumn *a priori* measurements, bathymetric and telemetric data, has been developed and then adapted to operate in real-time in tandem with the acoustic receiver instrumentation deployed at sea - the AOBs. This software is written in MATLAB® based on matched-filed processing techniques, an acoustic propagation model (C-SNAP), and a genetic algorithm (GA). One of the main features of this software is its ability to distribute the calculations related to candidate models (acoustic model and fit) to other computer nodes in a network in order to speed up computations. During the

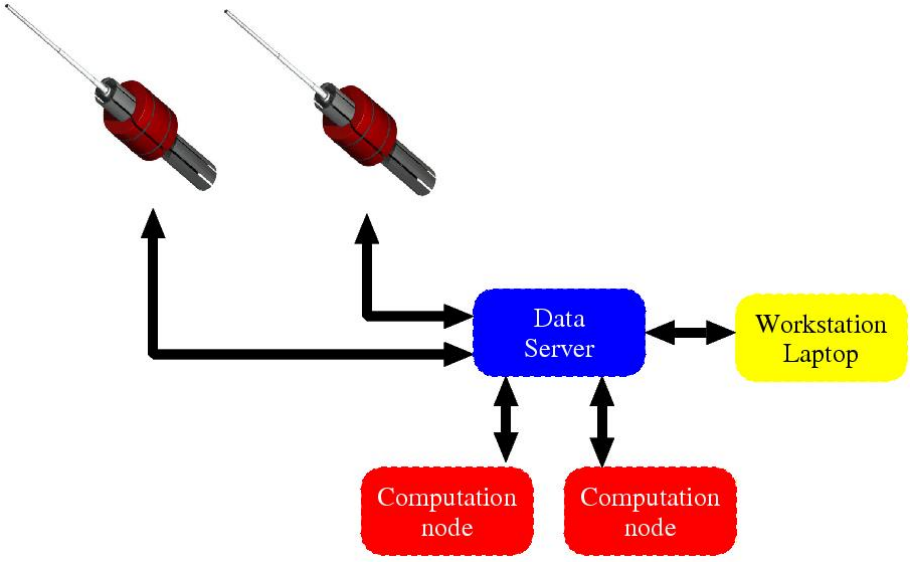

Figure 4.1: Simplified scheme describing the local network set up on NRV D. Carlos I during the RADAR'07 sea trial.

RADAR'07 the inversion software was running on the main data server. Its operation can be summarized in the following steps:

1. Lists the data files available in the selected AOB.

2. Download data files containing the sequence to be inverted. As the transmissions are precisely scheduled, it is accurately known which data files have to be downloaded.

3. Detect the beginning and extract time series. This was done by correlating the downloaded data with the probe inserted at the beginning of the emitted sequence (recall Fig. 3.3).

4. Based on GPS recordings of both the research vessel and the AOB position, a segmentation of the bathymetry is generated.

5. Then the GA that generates candidate models and performs global search of solutions is launched.

These models are distributed to the processing nodes, which compute the forward models in order to obtain the replicas, and yield the results of the comparison between model replicas and data. During the experiment the inversion code was set to alternately download acoustic data collected by both buoys. Day 192 was dedicated to solve a series of bugs that could not be detected during tests performed before the sea trial. During the remaing days the software remained stable without any failure.

4.2 Julian day 194: experimental results

In this section acoustic inversion results obtained during Julian day 194 are presented.

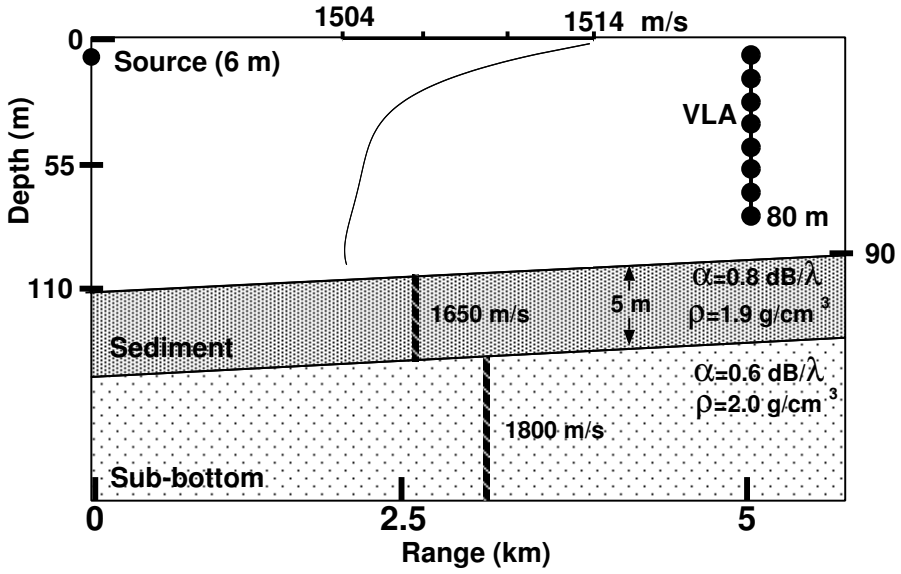

Figure 4.2: Baseline environmental model used for environmental inversion.

4.2.1 The experimental setup

On July 13 the two AOBs were deployed in a track with constant waterdepth of approximately 93 m. The research vessel towed the transmitting acoustic source and the AOBs drifted away from the deployment position as indicated by the GPS recordings in Fig. 2.17. The transmission tracks from time 10:52 to time 16:11 have a bathymetry with mild range-dependency. Afterwards, the source was towed to a position with a waterdepth decreasing down to 60 m, resulting in transmission tracks with very significant range-dependency. A waterdepth as low as 60 m may constitute a relatively severe condition in terms of modeling due to the strong interaction with the seafloor.

4.2.2 The environmental model

Figure 4.2 shows the baseline environmental model used for the environmental inversion. It consists of a three layer model with watercolumn, sediment layer, and sub-bottom. The watercolumn is modeled in terms of sound-speed according to the mean temperature profile, EOFs and mean salinity obtained from the oceanographic survey, and the properties for sediment and sub-bottom are respectively values typically found for sand and gravel. The waterdepth is based on the segmentation of the archival bathymetric information along the source-receiver cross sections at each time. For the purpose of inversion the parameter set consists of EOF coefficients α_1, α_2, and α_3, sediment parameters (sound velocity, density, thickness), sub-bottom sound velocity, and geometric parameters (source depth, receiver depth, array tilt). The parameters have different numbers of quantization step depending on the search interval resulting in a search space with dimension $\approx 7 \times 10^{16}$. Forward models are computed using the normal-mode acoustic propagation model C-SNAP [20].

4.2.3 The objective function

The environmental inversions are based on a Matched-Field Processing (MFP) technique [21]. Forward models for candidate parameter solutions are computed in order to obtain replica fields. These replica fields are compared to the acoustic field observation in order maximize the match. As direct inversion is not possible, neither exhaustive search, the inversion problem is posed as a global optimization problem. The comparison between field and replicas is performed by means of the Bartlett processor, given as

$$P(\underline{\theta}) = \sum_{k=1}^{K} \underline{H}^H(\underline{\theta}, \omega_k) \hat{\mathbf{C}}_{YY}(\omega_k) \underline{H}(\underline{\theta}, \omega_k), \tag{4.1}$$

where K is the number of discrete frequencies ω_k considered, $\underline{H}(\underline{\theta}, \omega_k)$ is the replica for the candidate parameter vector $\underline{\theta}$, and $\mathbf{C}_{YY}(\omega_k)$ is the sample spectral density matrix obtained by $\hat{\mathbf{C}}_{YY} = \frac{1}{N} \sum_{n=1}^{N} \mathbf{Y}_n \mathbf{Y}_n^H$. The present case considers tones with frequencies 500, 550, 600, 650, 700, and 800 Hz (hence $K = 6$), and a temporal window of 48 s divided into intervals of 1 s (hence $N = 48$). The parameter vector $\underline{\theta}$ that maximizes P gives the solution of the optimization problem. The search is performed using a genetic algorithm (GA).

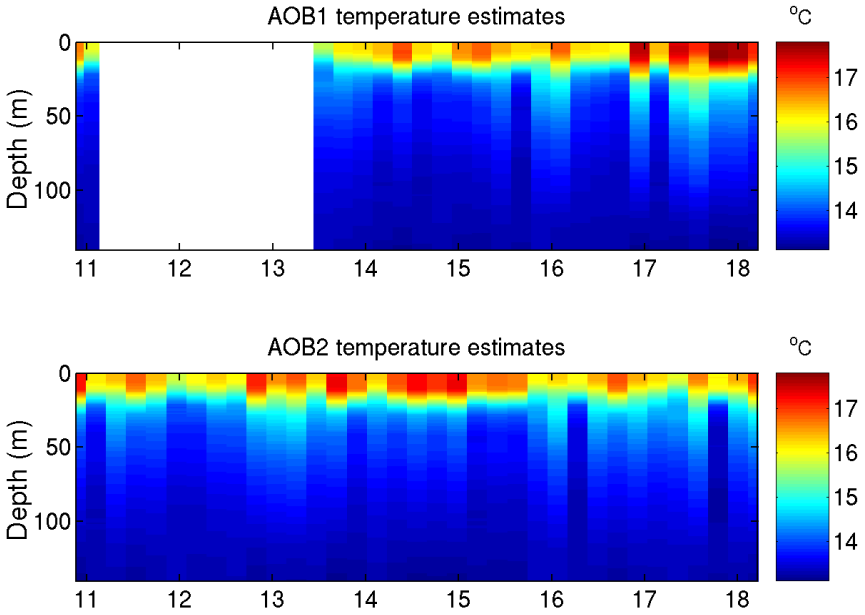

Figure 4.3: Baseline environmental model used for environmental inversion.

4.2.4 Online environmental inversion results

This section shortly presents the preliminary inversion results obtained with acoustic data received simultaneously on both AOBs during the sea trial. The primary objective of these inversions is to follow the variation of the temperature in the watercolumn in different ocean transects. Each data set was inverted at a rate of every 10 or every 20 minutes depending on computation load. Figure 4.3 shows the temperature estimates obtained. The estimated temperature profiles are relatively stable and the maximum values are in

line with the measurements obtained with thermistor chain of AOB22. In the bottom plot it appears that the decrease of temperature around time 12:00 UTC is detected, as a reduction of the surface temperature is obtained.

Chapter 5

Conclusions

The RADAR'07 sea trial took place in July 2007, off the west coast of Portugal in the Setúbal area. On board of the research vessel NRP D. Carlos I were three teams aiming at the transmission of acoustic signals for the following purposes:

- low-frequency acoustic tomography using multilple acoustic receiver arrays (UAlg team);
- high-frequency acoustic tomography (NURC team);
- underwater acoustic communications (UAlg and HLS Research teams).

The acoustic signals transmitted for the different purposes covered a frequency band from 0.5 to 20 kHz. This was possible thanks to the availability of three acoustic sources able to cover that band, and three signal generators. The different teams arranged schedules and transmissions in such a way that all transmitted simultaneously, by multiplexing signals in time and frequency, and by combibing waveforms into lineups containing those waveforms. At the other end three acoustic receiver arrays were used to collected the signals, the AOBs provided by UAlg, and the SLIVA array provided by NURC. The result was a very fruitful sea trial since a large amount of acoustic data was collected in a very efficient way.

The low-frequency acoustic data will mainly serve for continuing to develop concepts related to acoustic inversion for the estimation of environmental parameters using multiple acoustic receiver arrays, which is being called Networked Tomography. During the RADAR'07 the operational aspect of this concept has been successfully implemented, in an attempt to invert acoustic data collect only ten minutes before. This was possible thanks to the wireless communication facilities implemented in the AOBs that use standard internet data transfer protocols. The AOBs were part of a network of computers installed on the research vessel with no seams in between. The acoustic data could be downloaded from the AOBs to the server running the acoustic inversions provided during all times. It should be remarked that due to the length of the sequence used for the low-frequency tomography (45 s), generally three acoustic data files (72 s) had to be downloaded, which at some times took a significant time. These data were clearly oversampled since they were in a band up to a 1 kHz with a sampling frequency of 50000 samples per second. A decimation by a factor of ten would allow for significanty reduce downloading times, and in the case of multi-tones the data could be reduced to negligible amounts.

The high-frequency tomography data aims at verifying, across a fairly long period of time corresponding to one tidal cycle, the stability of the propagation for several bandwidths, signal durations and central frequencies for the same amount of energy produced, and, thus, obtain feasibility limits in terms of waveform frequency.

The underwater communications data transmitted jointly by UAlg and HLS Reasearch teams will be used to test high data rate communications (up to 2000 bits/s). The UAlg team is testing the possibility of using the passive time reversal concept in conjunction with an environmental equalizer that compensates the channel variability, e.g., induced by movements of the receivers in range and depth, or other causes. The HLS Research team is interested in comparing underwater communications with shallow and deep emitters. This is related to the fact that underwater communications are more difficult with shallow emitters than with deep emitters usually because the multi-path structure is more stable and focused at greater depths.

Appendix A

Detailed composition of individual files constructed by HLS Research

A.1 The HLS Research LF target sequence

This waveform was transmitted in the LF band during the High-Frequency Tomography phases of the experiment. It contained a number of broadband and narrowband signatures to be used for testing source tracking.

Unfortunately, the 500-4500 Hz used to form this waveform interfered with the lower edge of the MF band from 4000-8000 Hz. As soon as this was discovered during the first High-Frequency Tomography experiment phase, this waveform was modified by low pass filtering it to cut off at 4000 Hz. Subsequent LF waveforms, including the target-lf2 waveform described in the next section, were designed to stay below the 4000 Hz lower limit of the MF band. The LF target sequence has the following lineup:

- 1 second silence
- 0.5 to 4.5 kHz LFMs with 100 ms repeated every 150 ms, during 5 s
- 1 second silence
- 9 seconds m=11 m-sequences
- 0.25 seconds silence
- A 110 s tone combination with frequencies 1001, 1502, 2003, 2504, 3005, 3506, 4007
- 1 second silence
- 9 seconds m=11 m-sequences
- bi-polar m-sequences with 2047 symbols, repeated without gaps and completeted with a blank in order to complete 9 s
- 1 second silence
- A 210 second PRN sequence with carrier at 2.5 kHz, 3 kHz bandwidth, and a band excess of $\alpha = 0.32$

- 1 second silence

This lineup of waveforms has a total duration of 349 seconds, which is padded with a 1 second silent leader and a 10 second silent trailer to make a 6 minute file. This 6 minute waveform is concatenated behind the UAlg Networked Tomography 180 s waveform to make a 9 minute waveform. Some remarks:

- m-file `make_sc_lf.m` is used to modulate the m-sequences,
- m-file `make_prn2.m` is used to make 30 seconds of PRN waveform, which is then repeated 7 times (for 210 seconds),
- The raw PRN sequence is saved to MAT file `target_lf_prn.mat`.

For the low-frequency band, we use m-sequences with parameter $m = 11$. These sequences contain 2047 bi-polar symbols, which we transmit at a BPSK symbol rate of 3000 symbols/second, so 9 s contain 13 m-sequences.

A.2 The HLS Research LF2 target sequence

This waveform was transmitted in the LF band during the Probes & Comms and Networked Tomography phases of the experiment, and was intended to be used for testing source tracking in the *Field Calibration* work by HLS Research. `target-lf2` was a 60-second file using the 500-3500 Hz band. This was a correction to `target-lf`, which erroneously overlapped the designated 4-8 kHz mid-frequency band. `target-lf` covered the 500-4500 Hz band. Since the original `target-lf` had a duration of 349 seconds, which does not fit into any of the Probes & Comms or Networked Tomography schedules, the `target-lf2` file (described in this section) must have been used in place of `target-lf` throughout the Probes & Comms and Networked Tomography phases.

`target-lf2` contains the following lineup of waveforms:

- 1 second silence
- LFMs with 100 ms duration, 200 ms PRI, during 4 s completing 20 chirps
- 0.25 second silence
- A 25 seconds tone combination with 755, 806, 857, 908, 959, 1001, 1502, 2003, 2504, 3005, 3506
- 0.25 seconds silence
- LFMs with 100 ms duration, 200 ms PRI, during 4 s completing 20 chirps
- 0.25 second silence
- LFMs with 100 ms duration, 200 ms PRI, during 4 s completing 20 chirps
- 0.25 second silence

- A 25 second PRN sequence with carrier at 2.0 kHz, 2.25 kHz bandwidth, and a band excess of $\alpha = 0.32$
- 0.25 second silence

Some remarks:

- m-file `make_prn2.m` is used to construct the PRN waveform,
- The raw PRN sequence that was used to construct this waveform was saved to MAT file `target_lf2_prn.mat`,
- The latest LF file seems to have been the concatenation of the UAlg low tomography sequence 3 minutes file and six of the 60s waveforms described above (these files were produced by `target_lf2.m`).

A.3 The HLS Research MF target sequence

M-file target_mf.m produces a 59.5 sec file with the following lineup:

- 0.25 seconds silence
- LFMs (4-8kHz, 100 ms duration, 200 ms PRI, 4 seconds total or 20 chirps)
- 0.25 seconds silence
- m-sequences with $m = 11$; the number that can fit into 5 seconds are transmitted (without gaps), and the resulting waveform is padded with zeros out to the 5 second duration
- 0.25 seconds silence
- A 20 s tone combination with frequencies 4501, 5002, 5503, 6004, 6505, 7006, 7507
- 0.25 seconds silence
- LFMs with 100 ms duration, 200 ms PRI, during 4 s completing 20 chirps
- 0.25 seconds silence
- A 25 second PRN sequence with carrier at 6 kHz, 3 kHz bandwidth, and a band excess of $\alpha = 0.3$
- 0.25 second silence.

Some remarks:

- m-file `make_sc_mf.m` is used to modulate the m-sequences,
- the raw PRN sequence is saved to MAT file `target_mf_prn.mat`,

- the m-sequences contain 2047 chips (bi-polar BPSK symbols) occurring at a chip rate of 3000 chips/second, so 5 seconds contains 7 m-sequences. M-sequences have a particular auto-correlation property that results in their being excellent probe pulses, but this property can only be realized in a multipath environment if the channel spread is covered by multiple m-sequences, concatenated head-to-tail. Thus, these m-sequences have no gaps.

A.4 HF-PSK, HF-OFDM, HF-FSK-1, and HF-FSK-2 waveforms

The PSK and OFDM waveforms contain many variations of their respective modulation schemes, to be used to demonstrate adaptive modulation and to compare receiver algorithms. The PSK and OFDM waveforms consist of:

- BPSK, QPSK, and 8PSK modulations;
- turbo-codes with different puncturing schedules (to produce different code rates of 1/3, 1/2, 2/3, 3/4 and 7/8).

The PSK waveforms are divided into subbands, so that the symbol period relative to the expected channel time spread does require too many DFE equalizer taps to be practical. The OFDM waveforms use both cyclic prefix and zero-padding to limit inter-carrier interference. The FSK-1 and FSK-2 waveforms were two sets of Frequency Shift Keying waveforms, one with Hadamard coding and one without, to be used for an assessment of what this additional coding provides in terms of performance. These waveforms would take many pages to describe, which is a level of detail that is perhaps not appropriate for this report. Please contact HLS Research if full details are needed.

A.5 HF-probes waveform

The `make_hf_probe.m` m-file constructs waveform having following lineup:

- 0.25 seconds silence;
- 10 seconds LFMs (9-15 kHz, 100 ms long, repeated every 200 ms);
- 0.25 seconds silence;
- 49.0427 seconds of $m = 11$ m-sequences (4800 chips/second, 12 kHz carrier frequency, 20% excess bandwidth, additional low pass filter with stop band at 3 kHz);
- padded with silence so entire file is 60 seconds;

To calculate how many m-sequences fit into 49.0427 seconds, note that m-sequence with m=11 contain 2047 chips, and a chip rate of 4800 chips/second is being used. Thus, a single m-sequence will have length 2047/4800, which divided into 49.0427 seconds yields 115. The fact that this is a perfect integer is no surprise - `make_hf_probes.m` determines how many m-sequences can fit into the remaining space, and then pads the remainder with zeros. Note that in all cases, only complete m-sequences were concatenated head-to-tail.

A.6 lfm-mf and lfm-hf waveforms

The `lfm_mf.m` m-file constructs a waveform that consists of a 0.5 s second silent interval, 59 seconds of LFM chirps, and a 0.5 s second silent interval. The LFM chirps sweep the 4 to 8 kHz band, are 100 ms long, and are repeated every 300 ms (196 300 ms intervals fit into 59 seconds).

p_{LFM}	blank	blank
0.1 s	0.2 s	1.2 s
196×		1×

The description above is identical for the lfm-hf waveform, which lies in the 9 to 15 kHz band.

A.7 mseq-mf waveform

The `mseq_mf.m` m-file constructs a waveform consists of a 0.5 s second silent interval, roughly 59 seconds of consecutive $m = 11$ m-sequences at a symbol or chip rate of 3000 symbols/second, and a 0.5 s second silent interval at the end. M-file `make_sc_mf.m` applies a BPSK modulation to the bi-polar m-sequence using a symbol. A square-root raised cosine shaping filter with an excess bandwidth of 20% is used to upsample the data at baseband. The 3 kHz symbol band and its 20% excess bandwidth occupy 3.6 kHz. An additional filter uses the remaining 400 Hz as a transition band (preserving the shaping filter shape) to better isolate the designated 4 kHz band (4-8 kHz). The waveform is bandshifted to passband at a center frequency of 6 kHz. To calculate how many m-sequences fit into 59 seconds, note that an m-sequence with $m = 11$ contain 2047 bi-polar symbols which we are transmitting at a rate of 3000 symbols/second, so a single m-sequence will have length 2047/3000, which divided into 59 seconds yields 86.468. In all cases, only complete m-sequences were concatenated head-to-tail, so in this case 86 identical m-sequences were concatenated, and the remainder of the waveform was padded with zeros. Note that limiting the m-sequences to at most 59 seconds was to accommodate 0.5 s seconds of silence at the beginning and end of this waveform.

Appendix B

Files transmitted during the RADAR'07 sea trial

This chapter aims at listing the files used to construct the waveform lineups transmitted during the RADAR'07 sea trial.

B.1 Files transmitted during the Probes & Comms Deep Source transmissions

The 3 first columns of table B.1 show how how MF and HF components were combined to form stereo files for the Firebox, with the MF in one channel and the HF in the other. Column 1 has the MF files, column 2 has the HF files, and column 3 has the composite files.

MF file	HF file	Composite file	Length (min)
`ualg-mf.pcm`	`ualg-hf.pcm`	`UALG-mf-hf.pcm`	2
`target-mf.pcm`	`HF-PSK.pcm`	`hls-1.pcm`	1
`target-mf.pcm`	`HF-OFDM.pcm`	`hls-2.pcm`	1
`target-mf.pcm`	`HLS-FSK-1.pcm`	`hls-3.pcm`	1
`target-mf.pcm`	`HLS-FSK-2.pcm`	`hls-4pcm`	1
`target-mf.pcm`	`HF-probes.pcm`	`hls-567.pcm`	1

Table B.1: Files transmitted through MF and HF sources during the Probes & Communications experiment (source DEEP)

Some remarks:

- files `ualg-mf.pcm` and `ualg-hf.pcm` were provided by the UAlg team,
- m-file `target_mf.m` constructed file `target-mf.pcm`,
- files `HF-PSK.pcm`, `HF-OFDM-both.pcm`, `HLS-FSK-1.pcm`, and `HLS-FSK-2.pcm` contain waveforms corresponding to different acoustic communication schemes to be tested,

- m-file `make_hf_probe.m` was used to create `HF-probes.pcm`,
- m-file `target_mf.m` was used to construct `target-mf.pcm`,
- m-file `target_lf2.m` was used to construct `target-lf2.pcm`.

Individual MF and HF files were combined to form stereo composite files of duration 1 or 2 minutes, corresponding to the timeline shown in table B.1. These short-duration files were sequenced into a single 15-minute file called `ProbesComms-mf-hf.pcm` in the order shown below. The file played during the Probes & Communications experiment with MF and HF sources deep was file `PC-Deep-mf-hf.pcm` with the following lineup:

File name	Length (min)
`UALG-mf-hf.pcm`	2
`UALG-mf-hf.pcm`	2
`UALG-mf-hf.pcm`	2
`UALG-mf-hf.pcm`	2
`hls-1.pcm`	1
`hls-2.pcm`	1
`hls-3.pcm`	1
`hls-4.pcm`	1
`hls-567.pcm`	1
`hls-567.pcm`	1
`hls-567.pcm`	1

B.2 Files transmitted during the Probes & Communications Shallow Source transmissions

The make up of the composite files is shown in table B.2.

MF file	HF file	Composite file	Length (min)
`lfm-mf.pcm`	`HF-PSK.pcm`	`hls-8.pcm`	1
`mseq-mf.pcm`	`HF-OFDM-both.pcm`	`hls-9.pcm`	1
`lfm-mf.pcm`	`HLS-FSK-1.pcm`	`hls-10.pcm`	1
`mseq-mf.pcm`	`HLS-FSK-1.pcm`	`hls-11.pcm`	1

Table B.2: Pairs of files used to form the 1-minute stereo files for the shallow Probes & Communications transmissions. Note that only the combinations introduced for the Shallow Run are shown here (several of the combinations have already been described under the Deep Source Transmissions description)

.

The file transmitted during the Probes and Comms experiment when the source was SHALLOW is 'PC-Shallow-mf-hf.pcm'. This was formed by concatenating the following files (note the first four files are 2 minutes long, and the remaining files are 1 minutes long, making a total of 15 minutes).

File name	Length (min)
UALG-mf-hf.pcm	2
UALG-mf-hf.pcm	2
UALG-mf-hf.pcm	2
UALG-mf-hf.pcm	2
lfm-McCoy.pcm	1
hls-8.pcm	1
hls-9.pcm	1
hls-10.pcm	1
hls-11.pcm	1
hls-8.pcm	1
hls-9.pcm	1

B.3 Files transmitted during the Networked Tomography transmissions

The stereo file played through the PreSonus Firebox was NetworkTomo-mf-hf.pcm with the lineup of table B.3.

Left	Channel Right Channel	Stereo File	Length (min)
lfm-mseq-mf.pcm	ualg-hf	hls-probes-ualg-mf-hf.pcm	2
ualg-mf.pcm	hls-psk-ofdm-mf.pcm	ualg-mf-hls-psk-ofdm.pcm	2
ualg-mf.pcm	hls-fsk-mf.pcm	ualg-mf-hls-fsk.pcm	

Table B.3: Pairs of MF and HF waveform files combined to form composite stereo files for the Networked Tomography phase. Some of these 2-minute files were constructed from pairs of 1-minute files.

Some remarks:

- file lfm-mseq-mf.pcm is a combination of lfm-mf.pcm and mseq-mf.pcm;
- file hls-psk-ofdm-mf.pcm is a concatenation of files HF-PSK.pcm and HF-OFDM-both.pcm;
- file hls-fsk-mf.pcm is a concatenation of files HLS-FSK-1.pcm and HLS-FSK-2.pcm.

File NetworkTomo-mf-hf.pcm was the stereo (MF and HF) file used during the Networked Tomography phase of the experiment. This file was the concatenation of the following stereo files:

File name	Length (min)
`lfm-McCoy.pcm`	1
`hls-probes-ualg-mf-hf.pcm`	2
`hls-probes-ualg-mf-hf.pcm`	2
`hls-probes-ualg-mf-hf.pcm`	2
`hls-probes-ualg-mf-hf.pcm`	2
`lfm-McCoy.pcm`	1
`ualg-mf-hls-psk-ofdm.pcm`	2
`ualg-mf-hls-fsk.pcm`	2
`ualg-mf-hls-psk-ofdm.pcm`	2
`ualg-mf-hls-psk-ofdm.pcm`	2

Some remarks:

- The file `lfm-McCoy.pcm` is the pairing of MF and HF waveforms provided by McCoy from NURC;
- See descriptions of `lfm_mf.m` and `mseq_mf.m` for waveform parameters of HLS-lfm-m and HLS-mseq-m waveforms played through the MF source;
- `Ualg-PSK` waveforms were provided by the UAlg team;
- `Ualg-tomo` waveforms were provided by the UAlg team. These are the low-frequency probe signals that were used for Networked Tomography.

Appendix C

M-files used to construct HLS waveforms

C.1 The `construct_pc_mf_hf.m` m-file

The `construct_pc_mf_hf.m` m-file calls the `pc_merge.m` m-file to create a stereo file to play two digital waveforms simultaneously (to drive the MF and HF projectors with different waveforms, as shown in the lineups above). After creating a bunch of stereo files (consistent with the distinct combinations of MF and HF waveforms shown in the lineups above), m-file `concat_files.m` is called to concatenate the various stereo files to form a complete 15 or 24 minute cycle.

There are switches for each of the three lineups:

- Probes and comms, deep run: setting switch `deep_p` to 1 produces file `PC-deep-mf-hf.pcm`;
- Probes and comms, shallow run: setting switch `shallow_p` to 1 produces file `PC-shallow-mf-hf.pcm`;
- Networked tomography: setting switch `network_tomo_p` to 1 produces file `NetworkTomo-mf-hf.pcm`.

C.2 m-files to construct Multiple-Subband PSK waveforms

m-files `make_radar_psk_hf.m`, `make_radar_psk_mf.m`, and `make_radar_psk_lf.m` were used to create waveforms for the following modulation schemes and code rates:

	$\frac{1}{3}$	$\frac{1}{2}$	$\frac{2}{3}$	$\frac{3}{4}$
BPSK				
QPSK				
8PSK				

All codewords were encoded using turbo codes with different puncturing rates. The transmitted sample rate was 96000 Hz. Subbands of bandwidth 1000 Hz were used, with the following center frequencies in each of the low (1000 to 4000 Hz), mid (4000 to 8000 Hz) and high frequency bands (9000 to 15000 Hz):

1 - 4 kHz	1500, 2500, 3500
4 - 8 kHz	4500 5500 6500 7500
9 - 15 kHz	9500 10500 11500 12500 13500 14500

Each suband has essentially the same design, with each subband differing only in their final center frequency. The processing carried out to generate each subband is the same up to the bandshift with distinct center frequencies. The random channel interleaver was taken from MAT file `radar_channel_interleaver.mat`. A square root raised cosine shaping filter was used with excess bandwidth of 20%. This shaping filter was truncated at 6 symbols on each side (12 symbols total). M-file `codeword_get.m` was used to read the distinct codeword and turbo-interleaver for each distinct code rate. Codewords were the encoded packets of 4800 original information bits, having sizes that depended on the code rate used to encode them. For example, the number of encoded symbols produced from a packet of 4800 information bits using the rate $\frac{1}{3}$ code and QPSK modulation was 7200 symbols (2 bits/symbol so 2400 uncoded symbols, tripled to produce 7200 coded symbols using the rate $\frac{1}{3}$). m-files `BPSK_modulator.m`, `QPSK_modulator.m`, and `PSK8_modulator.m` were used to convert the codewords into constellation symbols. A sequence of ten symbols having value 1 preceded each codeword used. m-file `radar_psk.m` was used to upsample these coded symbol sequences to the sample frequency of the transmission system and bandshift them up to their center frequencies.

C.3 m-files to construct OFDM waveforms

OFDM files were constructed for the following combinations:

- Regular and differentially coded sequences.
- BPSK, QPSK, and 8PSK modulations schemes.l
- Code rates of $\frac{1}{2}$ and $\frac{3}{4}$.
- 1024 tones with 25% cyclic prefix, 1024 tones with 50% cyclic prefix, and 2048 tones with 25% cyclic prefix.

From these combinations, the following combinations were skipped to fit the sequence of combinations into the allowable time:

- HF_BPSK_1_2_1024_50.pcm;
- HF_BPSK_3_4_1024_50.pcm.

OFDM waveforms were constructed for the HF band only. m-file `radar_ofdm_hf.m` was used to construct pcm files for each combination of attributes above. The random

channel interleaver was read from MAT file `radar_channel_interleaver.mat`. m-file `codeword_get.m` was used to read codewords for each code rate. m-files `BPSK_modulator.m`, `QPSK_modulator.m`, and `PSK8_modulator.m` were used to convert the codewords into constellation symbols. m-file `generateOFDM.m` was used to produce the time series OFDM waveform by performing an IFFT on the set of modulated tones. This produces a time series interval corresponding to a complete FFT period. The cyclic prefix is added at the top level of m-file `radar_ofdm_hf.m`. The differentially encoded OFDM waveforms are similarly created using m-file `radar_ofdm_hf_diff.m` with the simple additional setp of using m-file `encode_differential.m` to convert the original sequence of modulated or constellation symbols to a differentially modulated sequence (each differentially modulated symbol is the complex product of the original symbol and its differentially modulated predecessor, with the output first symbol taken to be the unmodified original first symbol).

C.4 m-files for Probe waveforms

The following table contains a listing of m-files that generate probe waveform files:

m-file	waveform file
`make_hf_probe.m`	`HF-probes.pcm`
`lfm_mf.m`	`lfm-mf.pcm`
`mseq_mf.m`	`mseq-mf.pcm`

C.5 m-files for target waveforms

The following table contains a listing of m-files that generate target waveform files:

m-file	waveform file
`target_lf.m`	`target-lf.pcm`
`target_lf2.m`	`target-lf2.pcm`
`target_mf.m`	`target_mf.pcm`

C.6 m-files to modulate PSK sequences

C.6.1 The `radar_psk.m` m-file

The `radar_psk.m` m-file constructs multiple-subband PSK waveforms. The symbol sequence is upsampled by $N_s = 8$ and low pass filtered by shaping filter to produce a complex time series sampled at $f_{s,1} = N_s \times R_s$, or 6000 ($R_s = 750$ symbols/second). Note that the shaping filter has significant sidelobes that would interfere with neighboring subbands. Thus, an additional low pass filter (besides the shaping filter) is applied to (each) baseband signal before modulating it onto each of the carriers. This filter was designed as follows. Adjacent subband center frequencies are separated by 1000 Hz, such that we will choose to preserve a 900 Hz band (this retains some of the shaping filter). Half of

900 Hz is 450, and therefore the left edge of next subband up is 1000-450=550. Thus, we can design this filter with a cutoff frequency of 450 Hz and a stopband starting at 550 Hz (thus, leaving a 100 Hz transition band). The sample rate at which to design this filter is $N_s \times R_s$, or 6000 ($N_s = 8$ is the number of samples per symbol, and $R_s = 750$ is the symbol rate at baseband). At this point a shaping filter and band isolation filter have been applied, and info bits occupy the band -375 to 375 Hz, with excess bandwidth of 20% for the shaping filter whose spectrum occupies -450 to 450 Hz, and applied an additional low pass filter transition band from 450 to 550 Hz (from right edge of baseband band to left edge of next band up - with edges at band edges of shaping filter). Now we upsample once more by 16 to create the final baseband waveform, sampled at 96000 Hz. The low pass filter for this upsampling has a passband of 450 Hz and a stopband of 96000-450=95550 Hz. In an operational modem, different information bits would be modulated in each subband, so the entire process above would be repeated for each of the distinct information bit streams. However, for the RADAR'07 test, we used the same information bit stream in each subband, and then, after producing a baseband waveform containing this single info bit stream, we bandshifted this baseband waveform to each of the subband center frequencies and summed the results so that we had a single complex time series waveform containing all six subbands.

C.6.2 The `make_sc_lf.m` m-file

A bit sequence at rate 3000 symbols/second to be transmitted in band 4000 using shaping filter with excess bandwidth of 20%. Upsample baseband signal at rate 3000 by 8 up to 24000, using shaping filter to low-pass filter zero pad images. Now I want to tighten up the band by applying an additional low pass filter, whose pass band includes the shaping filter excess bandwidth of 1.2×3000 (pass-band frequency is 1.2×1500). The transition band of this final filter is determined by fact that neighboring band is centered at 4000 Hz, so stop band will start at $4000 - f_{\text{pass}}$ or $4000 - 1.2 \times 1500$. This requires a filter size of 500 coefficients at 24 kHz sample rate. Once the signal is suitably shaped in the frequency domain at 24 kHz, I upsample it again by 4 using `upfirdn.m`. This requires another low pass filter, with passband at 1.2×1500 and stopband at 24 kHz - 1.2×1500, which is a very easy filter (few coefficients) to design.

C.6.3 The `make_sc_mf.m` m-file

this text has the same frequency values as that above A bit sequence at rate 3000 symbols/second to be transmitted in band 4000 using shaping filter with excess bandwidth of 20%. Upsample baseband signal at rate 3000 by 8 up to 24000, using shaping filter to low-pass filter zero pad images. Now I want to tighten up the band by applying an additional low pass filter, whose pass band includes the shaping filter excess bandwidth of 1.2×3000 (pass-band frequency is 1.2×1500). The transition band of this final filter is determined by fact that neighboring band is centered at 4000 Hz, so stop band will start at $4000 - f_{\text{pass}}$ or $4000 - 1.2 \times 1500$. This requires a filter size of 500 coefficients at 24 kHz sample rate. Once the signal is suitably shaped in the frequency domain at 24 kHz, I upsample it again by 4 using `upfirdn.m`. This requires another low pass filter, with passband at 1.2×1500 and stopband at 24 kHz - 1.2×1500, which is a very easy filter (few coefficients) to design.

C.6.4 The `make_sc_hf.m` m-files

A bit sequence at rate 4800 symbols/second to be transmitted in band 6000 using shaping filter with excess bandwidth of 20%. Upsample baseband signal at rate 4800 by 5 up to 24000, using shaping filter to low-pass filter zero pad images. Now I want to tighten up the band by applying an additional low pass filter, whose pass band includes the shaping filter excess bandwidth of 1.2×4800 (pass-band frequency is 1.2×2400). The transition band of this final filter is determined by fact that neighboring band is centered at 4000 Hz, so stop band will start at $6000 - f_{\text{pass}}$ or $6000 - 1.2 \times 1500$. This requires a filter size of 500 coefficients at 24 kHz sample rate. Once the signal is suitably shaped in the frequency domain at 24 kHz, I upsample it again by 4 using `upfirdn.m`. This requires another low pass filter, with passband at 1.2×1500 and stopband at 24 kHz - 1.2×2400, which is a very easy filter (few coefficients) to design.

Appendix D

The `ReadVLAData.m` m-file

The `ReadVLAData.m` m-file is used to read the data files generated by the AOBs.

```
function [data, Fs, NoSs, TITLE, TIMEPOS] = ReadVLAData(filename, DataType)
%
% Reads a Data File from the AOB or ULVA DAQ System
%
%   [data, Fs, NoSs, TITLE, TIMEPOS] = ReadVLAData(filename, DataType)
%
% Where:
%     data: is a matrix [ NoChannels * Total No Samples ]
%     fs: sampling frequency
%     NoSs: Number of Channels
%     TITLE: Description of the experiment
%     TIMEPOS: Time/Position information of the data in the file
%
%     filename: complete filename to be read including extension.
%     DataType:  'acoustic' or 'nonacoustic'



if ( nargin < 2 )
  error('Two parameter are required\n Sintax: ReadLOCAPASSData(filename,...
         DataType);\n DataType must be "acoustic" or "nonaccoustic"');
end

disp(['Trying to open: ' filename ' !!!']);
fid = fopen(filename,'r');
if (fid==-1)
   error(['File:' filename 'could not be open!!']);
end
disp('File Openned!!');

TITLE = fgetl(fid);
teststr(TITLE);

TIMEPOS = fgetl(fid);
```

```
teststr(TIMEPOS);

NonAcdatainfo = fgetl(fid);
teststr(NonAcdatainfo);

Acdatainfo = fgetl(fid);
teststr(Acdatainfo);

switch DataType
case ['timeposition']
    data = [];
    count = 0;
    Fs   = str2num(NonAcdatainfo(16:20));       % Sampling frequency
    NoSs = str2num(NonAcdatainfo(29:30));       % No of Channels
    SpSz = str2num(NonAcdatainfo(39:40));       % No of Bits per Samples
    ToSp = str2num(NonAcdatainfo(47:54));       % Total Number of Samples
case ['nonacoustic'],
    Fs   = str2num(NonAcdatainfo(16:20));       % Sampling frequency
    NoSs = str2num(NonAcdatainfo(29:30));       % No of Channels
    SpSz = str2num(NonAcdatainfo(39:40));       % No of Bits per Samples
    ToSp = str2num(NonAcdatainfo(47:54));       % Total Number of Samples
    testinfo(Fs); testinfo(NoSs); testinfo(SpSz); testinfo(ToSp);
    if NoSs > 0
      [data count]=fread(fid,[NoSs ToSp/NoSs],['int' num2str(SpSz)]);
    else
       data = [];
       count = 0;
    end
case ['acoustic'],
    NoSs = str2num(NonAcdatainfo(29:30));       % No of Channels
    SpSz = str2num(NonAcdatainfo(39:40));       % No of Bits per Samples
    ToSp = str2num(NonAcdatainfo(47:54));       % Total Number of Samples
    if NoSs > 0
%skip NonAc data
      [data count]=fread(fid,[NoSs ToSp/NoSs],['int' num2str(SpSz)]);
    end
    Fs   = str2num(Acdatainfo(16:20));        % Sampling frequency
    NoSs = str2num(Acdatainfo(29:30));        % No of Channels
    SpSz = str2num(Acdatainfo(39:40));        % No of Bits per Samples
    ToSp = str2num(Acdatainfo(47:54));        % Total Number of Samples
    testinfo(Fs); testinfo(NoSs); testinfo(SpSz); testinfo(ToSp);
    [data count]=fread(fid,[NoSs ToSp/NoSs],['int' num2str(SpSz)]);
otherwise,
    fclose(fid);
    error('Wrong data type!')
end

disp('Data Read!')
disp('File Closed..')

if count < ToSp
   disp('Not a Full File!');
end
```

```
return


% ************************************************************************
% **********    Auxiliary Functions ***************************************
% ************************************************************************


function teststr(strarr)
if ~ischar(strarr)
   error('Not a Valid DATA file!!');
end
return

function testinfo(valuearr)
if isempty(valuearr)
   error('Not a Valid DATA file!!');
end
return

function out=gettype(strarr)

found=findstr(strarr,'.');
if isempty(found)
   error('No Filename extension!!!')
else
   out=strarr((found(end)+1):end);
end

return
```

Bibliography

[1] C. Soares, S. M. Jesus, and E. Coelho. Acoustic oceanographic buoy testing during the maritime rapid environmental assessment 2003 sea trial. In D. Simons, editor, *Proc. of European Conference on Underwater Acoustics 2004*, pages 271–279, Delft, Netherlands, 2004.

[2] A. Silva, F. Zabel, and C. Martins. Acoustic oceanographic buoy: a telemetry system that meets rapid environmental assessment requirements. *Sea-Technology*, 47(9):15–20, September 2006.

[3] S. Jesus, A. Silva, and C. Soares. Acoustic Oceanographic Buoy test during the MREA'03 sea trial. Internal Report Rep. 04/03, SiPLAB/CINTAL, Universidade do Algarve, Faro, Portugal, November 2003.

[4] S. Jesus, C. Soares, P. Felisberto, A. Silva, L. Farinha, and C. Martins. Acoustic Maritime Rapid Environmental Assessment during the MREA'04 sea trial. Internal Report Rep. 02/05, SiPLAB/CINTAL, Universidade do Algarve, Faro, Portugal, March 2005.

[5] C. Soares and S. M. Jesus. Matched-field tomography using an acoustic oceanographic buoy. In S. M. Jesus, editor, *Proc. of European Conference on Underwater Acoustics 2006*, pages 717–722, Carvoeiro, Portugal, 2006.

[6] N. Martins, C. Soares, and S. M. Jesus. Environmental and acoustic assessment: the aob concept. *Journal of Marine Systems*, 69:114–125, 2008.

[7] A. Silva, S. M. Jesus, and J. P. Gomes. Acoustic array depth and range shift compensation by using a waveguide invariant property. In *Proc. Underwater Acoustic Measurements*, pages 1315–1320, Heraklion, Greece, June 2007.

[8] A. Silva, S. M. Jesus, and J. P. Gomes. Passive time reversal probe-signal capture optimization for underwater communications. In *Proc. Underwater Acoustic Measurements*, pages 1371–1376, Heraklion, Greece, June 2007.

[9] A. Silva, S. Jesus, and J. P. Gomes. Physics-based passive time reversal equalizer using shallow water waveguide invariant properties. In *Proc. OCEANS'07*, Vancouver, October 2007.

[10] J. P. Gomes, A. Silva, and S. Jesus. Joint passive time reversal and multichannel equalization for underwater communications. In *OCEANS'06*, Boston (USA), September 2006.

[11] J. P. Gomes, A. Silva, and S. Jesus. Performance analysis of multichannel lattice equalization in coherent underwater communications. In *Proc. OCEANS'07*, Vancouver (Canada), October 2007.

[12] S. M. Jesus, C. Soares, E. Coelho, and P. Picco. An experimental demonstration of blind ocean acoustic tomography. *J. Acoust. Soc. Am.*, 3(119):1420–1431, March 2006.

[13] J. Small. Internal tide transformation across a continental slope off cape sines, portugal. *Journal of Marine Systems*, 32(1-3):43–69, 2002.

[14] M. Rixen and E. Ferreira-Coelho. Operational prediction of acoustic properties in the ocean using multi-model statistics. *Ocean Modelling*, 11:428–440, 2006.

[15] S. M. Jesus, A. Silva, , and C. Soares. INTIFANTE'00 sea trial data report - Events 1, 2 and 3. Data Report 02/01, SiPLAB, Faro, Portugal, 2001.

[16] R. Haynes, E. D. Barton, and I. Pilling. Development, persistence and variability of upwelling filaments off the atlantic coast of the iberian peninsula. *J. Geophys. Res.*, 98(C12):22681–22692, 1993.

[17] F. Zabel and C. Martins. RBR Thermistors array for AOB2. Internal Report Rep. 04/06, University of Algarve, Faro, Portugal, September 2006.

[18] A. Silva, C. Martins, and S. M. Jesus. Acoustic oceanographic buoy (version 1). Internal Report Rep. 03/05, SiPLAB/CINTAL, Universidade do Algarve, Faro, Portugal, October 2005.

[19] F. Zabel, C. Martins, and A. Silva. Acoustic Oceanographic Buoy (version 2). Internal Report Rep. 05/05, University of Algarve, Faro, Portugal, 2005.

[20] C. M. Ferla, M. B. Porter, and F. B. Jensen. C-SNAP: Coupled SACLANTCEN normal mode propagation loss model. Memorandum SM-274, SACLANTCEN Undersea Research Center, La Spezia, Italy, 1993.

[21] A. Tolstoy. *Matched Field Processing for Underwater Acoustics*. World Scientific, Singapore, 1993.